Axial-vector transition form factors of the singly heavy baryons

Jung-Min Suh[1,*] and Hyun-Chul Kim[1,2,†]

[1]*Department of Physics, Inha University, Incheon 22212, Republic of Korea*
[2]*School of Physics, Korea Institute for Advanced Study (KIAS), Seoul 02455, Republic of Korea*

(Received 2 May 2022; accepted 31 October 2022; published 28 November 2022)

We investigate the axial-vector transition form factors of the lowest-lying singly heavy baryons within the framework of the chiral quark-soliton model. We consider the linear m_s corrections, dealing with the strange current quark mass m_s as a small perturbation. Since we have various relations between different transitions because of isospin symmetry and flavor SU(3) symmetry breaking, only two axial-vector transition form factors are independent. We present the numerical results for these form factors. The effects of the flavor SU(3) symmetry breaking turn out tiny, so we neglect them. We also compute the decay rates for several strong decays of the singly heavy baryons and compare the results with the experimental data and those from other models. While the results for the $\Sigma_c \to \Lambda_c^+ + \pi$ and $\Sigma_c^* \to \Lambda_c^+ + \pi$ decays are slightly overestimated in comparison with the corresponding experimental data, those for the $\Xi_c^* \to \Xi_c + \pi$ are in remarkable agreement with the data.

DOI: 10.1103/PhysRevD.106.094028

I. INTRODUCTION

The structure of singly heavy baryons has been much less known than that of the light baryons, both experimentally and theoretically. Even for the charmed baryons in the ground states, we know only their masses and decay widths [1]. Recently, the electromagnetic properties of the singly heavy baryons have been investigated within lattice QCD [2–5]. There have also been various theoretical works on their electromagnetic structure. On the other hand, there are very few works on the axial-vector properties of the singly heavy baryons. Since the LHCb Collaborations have continuously announced a series of new experimental data on the heavy baryons [6–13], one may expect that future experiments will reveal the axial-vector structure of the heavy baryons.

A singly heavy baryon consists of a heavy quark and two light quarks. In the limit of the infinitely heavy-quark mass ($m_Q \to \infty$), the spin of the heavy quark $\boldsymbol{S}_Q$ is conserved, which brings about the conservation of the spin of the light-quark degrees of freedom: $\boldsymbol{S}_{\rm L} \equiv \boldsymbol{S} - \boldsymbol{S}_Q$ [14–16]. It is called the heavy-quark spin symmetry, which allows one to take the total spin of the light quarks as a good quantum number. Thus, we can classify the singly heavy charmed baryons in the ground states according to the representation of flavor $SU(3)_{\rm f}$ symmetry: $\mathbf{3} \otimes \mathbf{3} = \bar{\mathbf{3}} \oplus \mathbf{6}$, where the baryon antitriplet ($\bar{\mathbf{3}}$) has $S_{\rm L} = 0$ and $S = 1/2$, whereas the baryon sextet ($\mathbf{6}$) carries $S_{\rm L} = 1$. Since the spin of the heavy quark is coupled to $\boldsymbol{S}_L$, the baryon sextet have two degenerate representations with $S = 1/2$ and $S = 3/2$, respectively, as illustrated in Fig. 1. This degeneracy is removed by introducing the color hyperfine interaction in order $1/m_Q$.

In the limit $m_Q \to \infty$, we regard the heavy quark inside a heavy baryon as a static color source, so the light quarks govern the structure of the singly heavy baryons. Some years ago, Yang *et al.* [17] proposed a pion mean-field approach to explain the masses of singly heavy baryons, following the idea proposed by Ref. [18]. Witten showed in his seminal papers [19,20] that in the limit of the large number of colors ($N_c \to \infty$) a baryon arises as a bound state of N_c *valence* quarks in a pion mean field with a hedgehog symmetry [21,22] that is a minimal extension of spherical symmetry with the characteristics of the pions considered. Since the quantum fluctuation around the saddle point of the pion field is suppressed by $1/N_c$ factor, one can ignore it. In this large N_c limit, the presence of N_c valence quarks that constitute the lowest-lying baryons causes the vacuum polarization, which creates the pion mean field. This pion mean field makes *self-consistently* the N_c valence quarks bound. To keep the hedgehog symmetry preserved in the case of flavor $\mathrm{SU}(3)_{\rm f}$, an SU(2) soliton is embedded into the isospin corner of $\mathrm{SU}(3)_{\rm f}$ [20].

The chiral quark-soliton model (χQSM) [23–25] was constructed such that it realizes Witten's idea. Note that in the χQSM the right hypercharge $Y_R = N_c/3$ is constrained by the N_c valence quarks, which is distinguished from the

*suhjungmin@inha.edu
†hchkim@inha.ac.kr

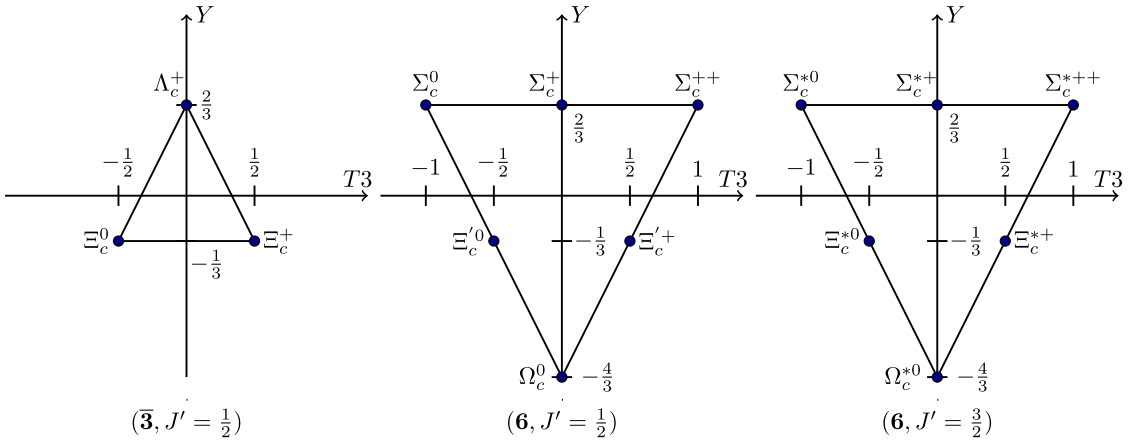

FIG. 1. Flavor $\mathrm{SU}(3)_\mathrm{f}$ representation of the singly heavy charmed baryons.

Skyrme model where the Wess-Zumino-Witten term fixes it. This indicates that the explicit valence quark degrees of freedom determine properly the baryon representations in the χQSM: This constrained right hypercharge selects allowed representations of light baryons such as the baryon octet (**8**), the decuplet (**10**), etc. The χQSM has a virtue because it can extend directly to describe singly heavy baryons. In the limit of $m_Q \to \infty$, a heavy quark inside the singly heavy baryon stays dormant but can play a role only as a static color source so that a colored soliton consisting of $N_c - 1$ valence quarks emerges. The right hypercharge $Y_R = (N_c - 1)/3$ is constrained by the $N_c - 1$ valence quarks, which picks the allowed representations of singly heavy baryons such as the baryon antitriplet ($\bar{\mathbf{3}}$) and the baryon sextet (**6**) as depicted in Fig. 1, and in addition the baryon antidecapentaplet ($\overline{\mathbf{15}}$) [26,27]. This extended χQSM have successfully applied in describing properties of the singly heavy baryons such as the mass splittings [17,28,29], isospin mass differences [30], magnetic moments [31], magnetic transitions and radiative decays [32], electromagnetic and radiative transition form factors [33–36], and gravitational form factors [37].

In the present work, we investigate the axial-vector transition form factors of the low-lying singly charmed baryons, including both the strangeness-conserving ($\Delta S = 0$) and strangeness-changing ($|\Delta S| = 1$) transitions. While there have been no theoretical works on the axial-vector transition form factors of singly heavy baryons, many theoretical groups studied their decay widths: for example, heavy hadron chiral perturbation theory (HHχPT) [38–41], a quark model (QM) [42], the light-front quark model (LFQM) [43], the relativistic three-quark model (RTQM) [44], the nonrelativistic constituent quark models (NRQM) [45,46], the $^3P_0$ strong decay model ($^3P_0$) [47], light cone QCD sum rules (LQCDSR) [48] and lattice QCD (LQCD) [49]. Since the heavy quark is not involved in the present axial-vector transitions of the singly heavy quarks, we can concentrate on the light quark degrees of freedom to compute the axial-vector transition form factors of the singly charmed baryons. We consider the rotational $1/N_c$ corrections and explicit breaking of $\mathrm{SU}(3)_\mathrm{f}$ symmetry to linear order [50]. Since we have already computed the axial-vector transition form factors of the baryon decuplet [51], we will focus on how the axial-vector transition form factors of the singly charmed baryons with spin $3/2$ behave differently from those of the Δ isobar.

The structure of the current work is summarized as follows: In Sec. II, we define the axial-vector transition form factors from the baryon sextet to both the baryon antitriplet and sextet, based on the transition matrix elements of the axial-vector current. In Sec. III, we show how to compute the axial-vector transition form factors of the singly heavy baryons in the χQSM. In Sec. IV, we first compare the present results with that of the $\Delta \to p$ axial-vector transition form factor. We then discuss the effects of $\mathrm{SU}(3)_\mathrm{f}$ symmetry breaking. The last section is devoted to summary and conclusions of the present work.

II. AXIAL-VECTOR TRANSITION FORM FACTORS BETWEEN THE SINGLY HEAVY BARYONS

The axial-vector current of a singly heavy baryon consists of the light-quark and heavy-quark parts:

$$A_\mu^\chi(x) = \bar{\psi}(x)\gamma_\mu\gamma_5\frac{\lambda^\chi}{2}\psi(x) + \bar{\Psi}(x)\gamma_\mu\gamma_5\Psi(x), \qquad (1)$$

where $\psi(x)$ represents the light-quark field $\psi = (u, d, s)$ in flavor space and $\Psi(x)$ denotes the heavy-quark field generically for the charm or bottom quark. The λ^χ denotes the well-known $\mathrm{SU}(3)_\mathrm{f}$ Gell-Mann matrices for which the index χ is determined by strangeness-conserving $\Delta S = 0$ transitions ($\chi = 1 \pm i2$) and for $|\Delta S| = 1$ ones ($\chi = 4 \pm i5$), respectively. Considering the Lorentz structure together with spin, parity, time reversal, and charge conjugation, we can parametrize the transition matrix elements of the axial-vector current between the baryons with spin $1/2$ in terms of two different real form factors:

$$\langle B'_{\frac{1}{2}}(p',J'_3)|A^{\chi}_{\mu}(0)|B_{\frac{1}{2}}(p,J_3)\rangle = \bar{u}(p',J'_3)\left[G_A^{(\chi)}(q^2)\gamma_\mu + \frac{G_P^{(\chi)}(q^2)}{M_{B'}+M_B}q_\mu\right]\frac{\gamma_5}{2}u(p,J_3), \quad (2)$$

where $G_A^{(\chi)}$ and $G_P^{(\chi)}$ are the axial-vector transition and pseudoscalar transition form factors of the corresponding baryon sextet with spin $1/2$, respectively. $u(p,J_3)$ and $\bar{u}(p',J'_3)$ stand for the Dirac spinors for the initial and final baryon states, respectively. M_B and $M_{B'}$ designate the corresponding masses, respectively. q_μ denotes the momentum transfer and q^2 its square. The transition matrix elements between the baryon with spin $3/2$ and with spin $1/2$ are parametrized in terms of four real form factors [52]:

$$\begin{aligned}\langle B'_{\frac{1}{2}}(p',J'_3)|A^{\chi}_{\mu}(0)|B_{\frac{3}{2}}(p,J_3)\rangle &= \bar{u}(p',J'_3)\left[\left\{\frac{C_3^{A(\chi)}(q^2)}{M_{B'}}\gamma^\nu + \frac{C_4^{A(\chi)}(q^2)}{M_{B'}^2}p^\nu\right\}(g_{\alpha\mu}g_{\rho\nu}-g_{\alpha\rho}g_{\mu\nu})q^\rho\right.\\ &\left. + C_5^{A(\chi)}(q^2)g_{\alpha\mu} + \frac{C_6^{A(\chi)}(q^2)}{M_{B'}^2}q_\alpha q_\mu\right]u^\alpha(p,J_3), \quad (3)\end{aligned}$$

where $g_{\alpha\beta}$ represents the metric tensor $g_{\alpha\beta} = \mathrm{diag}(1,-1,-1,-1)$. In the rest frame of a initial baryon, p^α, $u^\alpha(p,J_3)$ is the Rarita-Schwinger spinor that describes a baryon with spin $3/2$, carrying the momentum p and J_3, which can be described by the combination of the polarization vector and the Dirac spinor, $u^\alpha(p,J_3) = \sum_{i,s} C^{\frac{3}{2}J_3}_{1i\frac{1}{2}s}\epsilon_i^\alpha(p)u_s(p)$. It satisfies the Dirac equation and the auxiliary equations $p_\alpha u^\alpha(p,J_3) = 0$ and $\gamma_\alpha u^\alpha(p,J_3) = 0$ [53]. The momenta of the initial and final states p and p', and the momentum transfer are explicitly written as

$$p = (M,\mathbf{0}), \qquad p' = (E',-\boldsymbol{q}), \qquad q = (\omega_q,\boldsymbol{q}), \quad (4)$$

where $q^2 = -Q^2$ with $Q^2 > 0$. Thus, the three-vector momentum and energy of the momentum transfer are expressed by

$$\begin{aligned}|\vec{q}|^2 &= \left(\frac{M_B^2 + M_{B'}^2 + Q^2}{2M_B}\right)^2 - M_{B'}^2,\\ \omega_q &= \left(\frac{M_{B'}^2 - M_B^2 + Q^2}{2M_B}\right). \quad (5)\end{aligned}$$

The axial-vector transition form factor $G^{(\chi)}_{A,B\to B'}(Q^2)$ can be obtained in terms of the spatial parts of the axial-vector current in the spherical tensor form

$$\begin{aligned}G^{(\chi)}_{A,\,B\to B'}(Q^2) = -2\sqrt{\frac{M_{B'}}{E_{B'}+M_{B'}}}\Bigg[&\int d^3r j_0(|\boldsymbol{q}||\boldsymbol{r}|)\langle B'_{\frac{1}{2}}(p',S'_3)|A^{\chi}_{10}(\boldsymbol{r})|B_{\frac{1}{2}}(p,S_3)\rangle\\ &- \int d^3r j_2(|\boldsymbol{q}||\boldsymbol{r}|)\langle B'_{\frac{1}{2}}(p',S'_3)|\{Y_2\otimes A^{\chi}_1(\boldsymbol{r})\}_{10}|B_{\frac{3}{2}}(p,S_3)\rangle\Bigg]. \quad (6)\end{aligned}$$

Since the form factor $C^{A(\chi)}_{5,B\to B'}(q^2)$ is the most dominant one, we concentrate on it. Its expression is very similar to Eq. (6)

$$\begin{aligned}C^{A(\chi)}_{5,\,B\to B'}(Q^2) = -\sqrt{\frac{2M_{B'}}{E_{B'}+M_{B'}}}\Bigg[&\int d^3r j_0(|\boldsymbol{q}||\boldsymbol{r}|)\langle B'_{\frac{1}{2}}(p',S'_3)|A^{\chi}_{10}(\boldsymbol{r})|B_{\frac{3}{2}}(p,S_3)\rangle\\ &- \int d^3r j_2(|\boldsymbol{q}||\boldsymbol{r}|)\langle B'_{\frac{1}{2}}(p',S'_3)|\{Y_2\otimes A^{\chi}_1(\boldsymbol{r})\}_{10}|B_{\frac{3}{2}}(p,S_3)\rangle\Bigg]. \quad (7)\end{aligned}$$

Note that $G^{(\chi)}_{A,B\to B'}(0)$ and $C^{A(\chi)}_{5,B\to B'}(0)$ are related to the strong coupling constants $g_{\pi BB'}$ by the Goldberger-Treiman relations.

III. A SINGLY HEAVY BARYON IN THE CHIRAL QUARK-SOLITON MODEL

The χQSM has proved great merit by showing that it can describe both the light and singly heavy baryons on the same footing. Since we want to discuss the axial-vector transition form factors of the singly heavy baryons in this work, we will first explain how a singly heavy baryon can be formulated in the pion mean-field approach. Let us define the normalization of the baryon state as $\langle B(p',J'_3)|B(p,J_3)\rangle = 2p_0\delta_{J'_3J_3}(2\pi)^3\delta^{(3)}(\boldsymbol{p}'-\boldsymbol{p})$. In the large N_c limit, this normalization is reduced to $\langle B(p',J'_3)|B(p,J_3)\rangle = 2M_B\delta_{J'_3J_3}(2\pi)^3\delta^{(3)}(\boldsymbol{p}'-\boldsymbol{p})$, where M_B is a baryon mass. A singly heavy baryon consists of the N_c-1 valence quarks and a static heavy quark, so the corresponding state can be written in terms of the Ioffe-type current of the N_c-1 valence quarks and a heavy-quark field in Euclidean space as follows:

$$|B,p\rangle = \lim_{x_4\to-\infty}\exp(ip_4x_4)\mathcal{N}(\boldsymbol{p})\int d^3x\exp(i\boldsymbol{p}\cdot\boldsymbol{x})(-i\Psi_h^\dagger(\boldsymbol{x},x_4)\gamma_4)J_B^\dagger(\boldsymbol{x},x_4)|0\rangle,$$
$$\langle B,p| = \lim_{y_4\to\infty}\exp(-ip_4'y_4)\mathcal{N}^*(\boldsymbol{p}')\int d^3y\exp(-i\boldsymbol{p}'\cdot\boldsymbol{y})\langle 0|J_B(\boldsymbol{y},y_4)\Psi_h(\boldsymbol{y},y_4), \tag{8}$$

where $\mathcal{N}(\boldsymbol{p})(\mathcal{N}^*(\boldsymbol{p}'))$ represents the normalization factor depending on the initial (final) momentum. $J_B(x)$ and $J_B^\dagger(y)$ stand for the Ioffe-type current consisting of the N_c-1 valence quarks [23] defined by

$$J_B(x) = \frac{1}{(N_c-1)!}\epsilon_{\alpha_1\cdots\alpha_{N_c-1}}\Gamma^{f_1\cdots f_{N_c-1}}_{(TT_3Y)(JJ_3Y_R)}\psi_{f_1\alpha_1}(x)\cdots\psi_{f_{N_c-1}\alpha_{N_c-1}}(x),$$
$$J_B^\dagger(y) = \frac{1}{(N_c-1)!}\epsilon_{\alpha_1\cdots\alpha_{N_c-1}}\Gamma^{f_1\cdots f_{N_c-1}}_{(TT_3Y)(JJ_3'Y_R)}(-i\psi^\dagger(y)\gamma_4)_{f_1\alpha_1}\cdots(-i\psi^\dagger(y)\gamma_4)_{f_{N_c-1}\alpha_{N_c-1}}, \tag{9}$$

where $f_1\cdots f_{N_c-1}$ and $\alpha_1\cdots\alpha_{N_c-1}$ denote respectively the spin-isospin and color indices. $\Gamma_{(TT_3Y)(JJ_3Y_R)}$ correspond to matrices with the quantum numbers $(TT_3Y)(JJ_3Y_R)$ for a given state. In the χQSM, right hypercharge Y_R is constrained by the number of the valence quarks while it is fixed by the Wess-Zumino-Witten term in the Skyrme model. It provides a distinct advantage for the χQSM, since the right hypercharge Y_R for singly heavy baryons is determined by the N_c-1 valence quarks: $Y_R = (N_c-1)/3$. The right hypercharge $Y_R = 2/3$ with $N_c = 3$ grants the baryon antitriplet ($\bar{\mathbf{3}}$), sextet ($\mathbf{6}$), antipentadecaplet ($\overline{\mathbf{15}}$), and so on [17,26,27,54]. $\psi_{f_k\alpha_k}(x)$ is the light-quark field. $\Psi_h(x)$ denotes the heavy-quark field, making the singly heavy baryon a color singlet. In the limit of $m_Q\to\infty$, the singly heavy baryon complies with the heavy-quark flavor symmetry, so that the heavy-quark field can be written as

$$\Psi_h(x) = \exp(-im_Qv\cdot x)\tilde{\Psi}_h(x). \tag{10}$$

Here $\tilde{\Psi}_h(x)$ stands for a rescaled heavy-quark field almost on mass-shell. It carries no information on the heavy-quark mass in the leading-order approximation in the heavy-quark expansion. v is the velocity of the heavy quark [14,15] with the superselection rule [16].

We now show the normalization factor $\mathcal{N}^*(\boldsymbol{p}')\mathcal{N}(\boldsymbol{p})$ to be $2M_B$. The normalization of the baryon state can be computed as follows:

$$\begin{aligned}\langle B(p',J_3')|B(p,J_3)\rangle &= \frac{1}{\mathcal{Z}_{\rm eff}}\mathcal{N}^*(p')\mathcal{N}(p)\lim_{x_4\to-\infty}\lim_{y_4\to\infty}\exp\left(-iy_4p_4'+ix_4p_4\right)\\
&\times\int d^3xd^3y\exp(-i\boldsymbol{p}'\cdot\boldsymbol{y}+i\boldsymbol{p}\cdot\boldsymbol{x})\int\mathcal{D}U\mathcal{D}\psi\mathcal{D}\psi^\dagger\mathcal{D}\tilde{\Psi}_h\mathcal{D}\tilde{\Psi}_h^\dagger\\
&\times J_B(y)\Psi_h(y)(-i\Psi_h^\dagger(x)\gamma_4)J_B^\dagger(x)\\
&\times\exp\left[\int d^4z\{(\psi^\dagger(z))_\alpha^f(i\partial\!\!\!/+iMU^{\gamma_5}+i\hat{m})_{fg}\psi^{g\alpha}(z)+\Psi_h^\dagger(z)v\cdot\partial\Psi_h(z)\}\right]\\
&= \frac{1}{\mathcal{Z}_{\rm eff}}\mathcal{N}^*(p')\mathcal{N}(p)\lim_{x_4\to-\infty}\lim_{y_4\to\infty}\exp\left(-iy_4p_4'+ix_4p_4\right)\\
&\times\int d^3xd^3y\exp(-i\boldsymbol{p}'\cdot y+i\boldsymbol{p}\cdot\boldsymbol{x})\langle J_B(y)\Psi_h(y)(-i\Psi_h^\dagger(x)\gamma_4)J_B^\dagger(x)\rangle_0,\end{aligned} \tag{11}$$

where $\mathcal{Z}_{\rm eff}$ represents the low-energy effective QCD partition function with the quark fields integrated out

$$\mathcal{Z}_{\rm eff} = \int\mathcal{D}U\exp(-S_{\rm eff}). \tag{12}$$

$\langle\ldots\rangle_0$ in Eq. (11) designates the vacuum expectation value of the baryon correlation function. $S_{\rm eff}$ is known as the effective chiral action (EχA) defined by

$$S_{\rm eff} = -N_c{\rm Tr}\ln[i\partial\!\!\!/+iMU^{\gamma_5}+i\hat{m}], \tag{13}$$

which embraces the effective nonlocal interaction between the quark and pseudo-Nambu-Goldstone (pNG) fields. M is the dynamical quark mass that arises from the spontaneous breakdown of chiral symmetry. The U^{γ_5} stands for the chiral field that is defined by

$$U^{\gamma_5}(z) = \frac{1-\gamma_5}{2}U(z) + U^\dagger(z)\frac{1+\gamma_5}{2} \tag{14}$$

with

$$U(z) = \exp[i\pi^a(z)\lambda^a], \tag{15}$$

where $\pi^a(z)$ represents the pNG fields and λ^a are the flavor Gall-Mann matrices. $\hat{m}$ displays the mass matrix of current quarks $\hat{m} = \mathrm{diag}(m_\mathrm{u}, m_\mathrm{d}, m_\mathrm{s})$. We regard the strange current quark mass m_s as a small perturbation.

The Green's function of a light quark in the χQSM [23] is given by

$$\begin{aligned} G(y,x) &= \langle y|\frac{1}{i\partial\!\!\!/ + iMU^{\gamma_5} + i\bar{m}}(i\gamma_4)|x\rangle \\ &= \Theta(y_4 - x_4)\sum_{E_n>0} e^{-E_n(y_4-x_4)}\psi_n(\boldsymbol{y})\psi_n^\dagger(\boldsymbol{x}) \\ &\quad - \Theta(x_4 - y_4)\sum_{E_n<0} e^{-E_n(y_4-x_4)}\psi_n(\boldsymbol{y})\psi_n^\dagger(\boldsymbol{x}), \end{aligned} \tag{16}$$

where $\Theta(y_4 - x_4)$ is the Heaviside step function. $\bar{m}$ denotes the average mass of the up and down current quarks: $\bar{m} = (m_\mathrm{u} + m_\mathrm{d})/2$ that constitutes an essential part in producing the correct Yukawa tail of the soliton profile function. E_n corresponds to the energy eigenvalue of the single-quark eigenstate given by

$$H\psi_n(\boldsymbol{x}) = E_n\psi_n(\boldsymbol{x}), \tag{17}$$

where H is the one-body Dirac Hamiltonian in the presence of the pNG boson fields, defined by

$$H = \gamma_4\gamma_i\partial_i + \gamma_4 MU^{\gamma^5} + \gamma_4\bar{m}\mathbf{1}. \tag{18}$$

The Green's function for the heavy quark in the limit of $m_Q \to \infty$ is given by the Heaviside step function and Dirac delta function

$$G_h(y,x) = \langle y|\frac{1}{\partial_4}|x\rangle = \Theta(y_4 - x_4)\delta^{(3)}(\boldsymbol{y} - \boldsymbol{x}), \tag{19}$$

which is the natural form of the heavy-quark propagator in the $m_Q \to \infty$ limit. Using these Green's functions for the light and heavy quarks and taking the limit of $y_4 - x_4 = T \to \infty$, we arrive at expression for the baryon correlation function $\langle J_B(y)\Psi_h(y)(-i\Psi_h^\dagger(x)\gamma_4)J_B^\dagger(x)\rangle_0$ [36]:

$$\begin{aligned} &\langle J_B(y)\Psi_h(y)(-i\Psi_h^\dagger(x)\gamma_4)J_B^\dagger(x)\rangle_0 \\ &\quad\sim \exp\left[-\{(N_c-1)E_\mathrm{val} + E_\mathrm{sea} + m_Q\}T\right] \\ &\quad= \exp[-M_B T]. \end{aligned} \tag{20}$$

Since the result for the correlation function given in Eq. (20) is canceled with the term $\exp(-iy_4p_4' + ix_4p_4) = \exp[M_B T]$ in the large N_c limit, i.e., $-ip_4' = -ip_4 = M_B = \mathcal{O}(N_c)$. Thus, the normalization factor is reduced to the mass of a singly heavy baryon: $\mathcal{N}^*(\boldsymbol{p}')\mathcal{N}(\boldsymbol{p}) = 2M_B$. Combining Eq. (20) with the normalization constant, we find that the classical mass of the singly heavy baryon is given by the sum of the $N_c - 1$ soliton and the heavy-quark masses

$$M_B = (N_c - 1)E_\mathrm{val} + E_\mathrm{sea} + m_Q, \tag{21}$$

which was already derived in a previous work [28]. The classical mass given in Eq. (21) comes into critical play, when we derive the axial-vector transition form factors of the singly heavy baryons, which will be mentioned in Sec. V.

IV. AXIAL-VECTOR TRANSITION FORM FACTORS IN THE CHIRAL QUARK-SOLITON MODEL

We now show how to compute the transition matrix elements of the axial-vector current (2), using the functional integral. Since the heavy quark is not involved, we will only consider the light quark degrees of freedom

$$\begin{aligned} \langle B(p', J_3')|A_\mu^a(0)|B(p, J_3)\rangle = \frac{1}{\mathcal{Z}}\lim_{T\to\infty}\exp\left(ip_4\frac{T}{2} - ip_4'\frac{T}{2}\right)\int d^3x d^3y\exp(-i\boldsymbol{p}'\cdot\boldsymbol{y} + i\boldsymbol{p}\cdot\boldsymbol{x}) \\ \int\mathcal{D}\pi^a\int\mathcal{D}\psi\int\mathcal{D}\psi^\dagger J_B(\boldsymbol{y}, T/2)\psi^\dagger(0)\gamma_4\gamma_\mu\gamma_5\frac{\lambda^a}{2}\psi(0)J_B^\dagger(\boldsymbol{x}, -T/2) \\ \times\exp\left[-\int d^4z(\psi^\dagger(z))_\alpha^f(i\partial\!\!\!/ + iMU^{\gamma_5} + i\hat{m})_{fg}\psi^{g\alpha}(z)\psi\right]. \end{aligned} \tag{22}$$

In the large-N_c limit, we use the saddle-point approximation to get the classical soliton. However, we have to take into account the zero modes that do not change the energy of the soliton. The angular velocity of the soliton.

Since the angular velocities of the soliton are of order $1/N_c$, we can deal with the angular velocities as a perturbative parameter. The integral over the translational zero modes in the leading order provides naturally the Fourier transform, which means that the baryon state has the proper translational symmetry. Thus, the functional integral over the pNG field is reduced to ordinary integrals over the zero modes. We also regard the strange current quark mass

m_s as a perturbation. Having performed the zero-mode quantization, we obtain the collective Hamiltonian as follows:

$$H_{\rm coll} = H_{\rm sym} + H_{\rm sb}, \tag{23}$$

where

$$H_{\rm sym} = M_{\rm cl} + \frac{1}{2I_1}\sum_{i=1}^{3}\hat{J}_i^2 + \frac{1}{2I_2}\sum_{p=4}^{7}\hat{J}_p^2,$$
$$H_{\rm sb} = \alpha D_{88}^{(8)} + \beta\hat{Y} + \frac{\gamma}{\sqrt{3}}\sum_{i=1}^{3}D_{8i}^{(8)}\hat{J}_i, \tag{24}$$

where I_1 and I_2 are the moments of inertia for the classical soliton and $D_{ab}^{(8)}$ is the SU(3) Wigner D function. The inertial parameters α, β and γ, which break flavor SU(3) symmetry explicitly, are written in terms of the moments of inertia I_1 and I_2, and the anomalous moments of inertia K_1 and K_2

$$\alpha = \left(-\frac{\bar{\Sigma}_{\pi N}}{3\bar{m}} + \frac{K_2}{I_2}\bar{Y}\right)m_s, \qquad \beta = -\frac{K_2}{I_2}m_s,$$
$$\gamma = 2\left(\frac{K_1}{I_1} - \frac{K_2}{I_2}\right)m_s, \tag{25}$$

where $\bar{\Sigma}_{\pi N}$ is related to the pion-nucleon Σ term: $\bar{\Sigma}_{\pi N} = (N_c - 1)N_c^{-1}\Sigma_{\pi N}$. As mentioned previously, the right hypercharge $\bar{Y}$ is fixed by the number of valence quarks, i.e., $Y_R = (N_c - 1)/3 = 2/3$. Diagonalizing the collective Hamiltonian, we derive the collective wave functions of the singly heavy baryon

$$\psi_B^{(\mathcal{R})}(J', J_3'; A) = \sum_{m_3=\pm 1/2} C^{J'J_3'}_{J_Q m_3 J J_3}\sqrt{\dim(p,q)}(-1)^{-\frac{\bar{Y}}{2}+J_3} \times D^{(\mathcal{R})*}_{(Y,T,T_3),(\bar{Y},J,-J_3)}(A)\chi_{m_3}, \tag{26}$$

where $C^{J'J_3'}_{J_Q m_3 J J_3}$ denotes the Clebsch-Gordan coefficient for the coupling between the collective light-quark wave function and the heavy-quark spinor χ_{m_3}. $\dim(p,q)$ represents the dimension of the (p,q) representation

$$\dim(p,q) = (p+1)(q+1)\left(1 + \frac{p+q}{2}\right). \tag{27}$$

In the presence of the flavor SU(3) symmetry breaking term $H_{\rm sb}$, the collective wave functions of the baryon sextet should be mixed with those in higher representations. Thus, the collective wave functions for the baryon antitriplet and sextet are obtained respectively as

$$|B_{\bar{\mathbf{3}}_0}\rangle = |\bar{\mathbf{3}}_0, B\rangle + p^B_{\overline{15}}|\overline{\mathbf{15}}_0, B\rangle, \tag{28}$$

$$|B_{\mathbf{6}_1}\rangle = |\mathbf{6}_1, B\rangle + q^B_{\overline{15}}|\overline{\mathbf{15}}_1, B\rangle + q^B_{\overline{24}}|\overline{\mathbf{24}}_1, B\rangle \tag{29}$$

with the mixing coefficients

$$p^B_{\overline{15}} = p_{\overline{15}}\begin{bmatrix}-\sqrt{15}/10\\ -3\sqrt{5}/20\end{bmatrix},$$
$$q^B_{27} = q_{\overline{15}}\begin{bmatrix}\sqrt{5}/5\\ \sqrt{30}/20\\ 0\end{bmatrix}, \quad q^B_{\overline{24}} = q_{\overline{24}}\begin{bmatrix}-\sqrt{10}/10\\ -\sqrt{15}/10\\ -\sqrt{15}/10\end{bmatrix}, \tag{30}$$

respectively, in the basis of $[\Lambda_c^+, \Xi_c]$ for the baryon antitriplet and $[\Sigma_c(\Sigma_c^*), \Xi_c'(\Xi_c^*), \Omega_c^0(\Omega_c^{*0})]$ for the baryon sextet. The parameters $p_{\overline{15}}$, $q_{\overline{15}}$ and $q_{\overline{24}}$ are given in terms of the inertia parameters α and γ

$$p_{\overline{15}} = \frac{3}{4\sqrt{3}}\alpha I_2, \qquad q_{\overline{15}} = -\frac{1}{\sqrt{2}}\left(\alpha + \frac{2}{3}\gamma\right)I_2,$$
$$q_{\overline{24}} = \frac{4}{5\sqrt{10}}\left(\alpha - \frac{1}{3}\gamma\right)I_2. \tag{31}$$

It is straightforward to compute the transition matrix elements of the collective states, which will be expressed by the SU(3) Clebsch-Gordan coefficients. So, we arrive at the final expressions for the axial-vector transition form factors of the singly heavy baryon with spin $1/2$ and $3/2$, respectively

$$G^{(\chi)}_{A,B\to B'}(Q^2) = \sqrt{2}\Bigg[\frac{\langle D^{(8)}_{a3}\rangle}{3}\{\mathcal{A}_0^{B\to B'}(Q^2) - \mathcal{A}_2^{B\to B'}(Q^2)\} - \frac{i\langle D^{(8)}_{a3}\rangle}{6I_1}\{\mathcal{D}_0^{B\to B'}(Q^2) - \mathcal{D}_2^{B\to B'}(Q^2)\}$$
$$+ \frac{1}{3\sqrt{3}I_1}\left[\langle D^{(8)}_{a8}\hat{J}_3\rangle + \frac{2m_s}{\sqrt{3}}K_1\langle D^{(8)}_{83}D^{(8)}_{a8}\rangle\right]\{\mathcal{B}_0^{B\to B'}(Q^2) - \mathcal{B}_2^{B\to B'}(Q^2)\}$$
$$+ \frac{d_{pq3}}{3I_2}\left[\langle D^{(8)}_{ap}\hat{J}_q\rangle + \frac{2m_s}{\sqrt{3}}K_2\langle D^{(8)}_{ap}D^{(8)}_{8q}\rangle\right]\{\mathcal{C}_0^{B\to B'}(Q^2) - \mathcal{C}_2^{B\to B'}(Q^2)\}$$
$$+ \frac{2m_s}{9}(\langle D^{(8)}_{a3}\rangle - \langle D^{(8)}_{88}D^{(8)}_{a3}\rangle)\{\mathcal{H}_0^{B\to B'}(Q^2) - \mathcal{H}_2^{B\to B'}(Q^2)\} - \frac{2m_s}{9}\langle D^{(8)}_{83}D^{(8)}_{a8}\rangle\{\mathcal{I}_0^{B\to B'}(Q^2) - \mathcal{I}_2^{B\to B'}(Q^2)\}$$
$$- \frac{2m_s}{3\sqrt{3}}d_{pq3}\langle D^{(8)}_{ap}D^{(8)}_{8q}\rangle\{\mathcal{J}_0^{B\to B'}(Q^2) - \mathcal{J}_2^{B\to B'}(Q^2)\}\Bigg], \tag{32}$$

$$
\begin{aligned}
C^{A(\chi)}_{5,B\to B'}(Q^2) = \sqrt{3}\Bigg[&\frac{\langle D^{(8)}_{a3}\rangle}{3}\{\mathcal{A}^{B\to B'}_0(Q^2)-\mathcal{A}^{B\to B'}_2(Q^2)\}-\frac{i\langle D^{(8)}_{a3}\rangle}{6I_1}\{\mathcal{D}^{B\to B'}_0(Q^2)-\mathcal{D}^{B\to B'}_2(Q^2)\}\\
&+\frac{1}{3\sqrt{3}I_1}\left[\langle D^{(8)}_{a8}\hat{J}_3\rangle+\frac{2m_s}{\sqrt{3}}K_1\langle D^{(8)}_{83}D^{(8)}_{a8}\rangle\right]\{\mathcal{B}^{B\to B'}_0(Q^2)-\mathcal{B}^{B\to B'}_2(Q^2)\}\\
&+\frac{d_{pq3}}{3I_2}\left[\langle D^{(8)}_{ap}\hat{J}_q\rangle+\frac{2m_s}{\sqrt{3}}K_2\langle D^{(8)}_{ap}D^{(8)}_{8q}\rangle\right]\{\mathcal{C}^{B\to B'}_0(Q^2)-\mathcal{C}^{B\to B'}_2(Q^2)\}\\
&+\frac{2m_s}{9}(\langle D^{(8)}_{a3}\rangle-\langle D^{(8)}_{88}D^{(8)}_{a3}\rangle)\{\mathcal{H}^{B\to B'}_0(Q^2)-\mathcal{H}^{B\to B'}_2(Q^2)\}\\
&-\frac{2m_s}{9}\langle D^{(8)}_{83}D^{(8)}_{a8}\rangle\{\mathcal{I}^{B\to B'}_0(Q^2)-\mathcal{I}^{B\to B'}_2(Q^2)\}\\
&-\frac{2m_s}{3\sqrt{3}}d_{pq3}\langle D^{(8)}_{ap}D^{(8)}_{8q}\rangle\{\mathcal{J}^{B\to B'}_0(Q^2)-\mathcal{J}^{B\to B'}_2(Q^2)\}\Bigg],
\end{aligned}
\tag{33}
$$

where $\langle\cdots\rangle$ designate the transition baryonic matrix elements of given collective operators. The explicit expressions for the quark densities $\mathcal{A}_{0,2}, \mathcal{B}_{0,2}, \mathcal{C}_{0,2}, \mathcal{D}_{0,2}, \mathcal{H}_{0,2}, \mathcal{I}_{0,2}$, and $\mathcal{J}_{0,2}$ can be found in Appendix A. Note that the corrections from flavor SU(3) symmetry breaking are originated from two different sources: that from the effective chiral action and that from the collective wave functions, which we denote them respectively as $(G^{(\chi)}_{A,B\to B'})^{(\mathrm{op})}$ and $(G^{(\chi)}_{A,B\to B'})^{(\mathrm{wf})}$

$$
G^{(\chi)}_{A,B\to B'}(Q^2) = (G^{(\chi)}_{A,B\to B'}(Q^2))^{(\mathrm{sym})} + (G^{(\chi)}_{A,B\to B'}(Q^2))^{(\mathrm{op})} + (G^{(\chi)}_{A,B\to B'}(Q^2))^{(\mathrm{wf})}. \tag{34}
$$

We decompose $C^{A(\chi)}_{5,B\to B'}$ in the same manner

$$
C^{A(\chi)}_{5,B\to B'}(Q^2) = (C^{A(\chi)}_{5,B\to B'}(Q^2))^{(\mathrm{sym})} + (C^{A(\chi)}_{5,B\to B'}(Q^2))^{(\mathrm{op})} + (C^{A(\chi)}_{5,B\to B'}(Q^2))^{(\mathrm{wf})}, \tag{35}
$$

where the detailed expressions for the SU(3)-symmetric part and symmetry-breaking parts can be found in Appendix B.

Scrutinizing Eqs. (B1)–(B6), we find isospin relations between different axial-vector transition form factors,

$$
\begin{aligned}
(\Xi_c'^{+}\to\Xi_c^{+}) &= -(\Xi_c'^{0}\to\Xi_c^{0}) = \frac{1}{\sqrt{2}}(\Xi_c'^{+}\to\Xi_c^{0}) = -\frac{1}{\sqrt{2}}(\Xi_c'^{0}\to\Xi_c^{+})\\
(\Sigma_c^{+}\to\Lambda_c^{+}) &= (\Sigma_c^{++}\to\Lambda_c^{+}) = (\Sigma_c^{0}\to\Lambda_c^{+})\\
(\Xi_c'^{+}\to\Lambda_c^{+}) &= (\Xi_c'^{0}\to\Lambda_c^{+})\\
(\Sigma_c^{++}\to\Xi_c^{+}) &= (\Sigma_c^{0}\to\Xi_c^{0}) = \sqrt{2}(\Sigma_c^{+}\to\Xi_c^{0}) = \sqrt{2}(\Sigma_c^{+}\to\Xi_c^{+})\\
(\Omega_c^{0}\to\Xi_c^{+}) &= -(\Omega_c^{0}\to\Xi_c^{0})\\
(\Sigma_c^{*++}\to\Sigma_c^{++}) &= -(\Sigma_c^{*0}\to\Sigma_c^{0}) = -(\Sigma^{*++}\to\Sigma_c^{+}) = (\Sigma_c^{*+}\to\Sigma_c^{++}) = -(\Sigma^{*+}\to\Sigma_c^{0}) = (\Sigma_c^{*0}\to\Sigma_c^{+})\\
(\Xi_c^{*+}\to\Xi_c'^{+}) &= -(\Xi_c^{*0}\to\Xi_c'^{0}) = \frac{1}{\sqrt{2}}(\Xi_c^{*0}\to\Xi_c'^{+}) = -\frac{1}{\sqrt{2}}(\Xi_c^{*+}\to\Xi_c'^{0})\\
(\Xi_c^{*0}\to\Sigma_c^{+}) &= -(\Sigma^{*+}\to\Xi_c'^{0}) = \frac{1}{\sqrt{2}}(\Xi_c^{*+}\to\Sigma_c^{++}) = -\frac{1}{\sqrt{2}}(\Sigma_c^{*++}\to\Xi_c'^{+}) = -(\Xi_c^{*+}\to\Sigma_c^{+})\\
&= -(\Sigma^{*+}\to\Xi_c'^{+}) = -\frac{1}{\sqrt{2}}(\Sigma^{*0}\to\Xi_c'^{+}) = \frac{1}{\sqrt{2}}(\Xi_c^{*0}\to\Sigma_c^{0})\\
(\Omega_c^{*0}\to\Xi_c'^{+}) &= -(\Xi_c^{*+}\to\Omega_c^{0}) = (\Omega_c^{*0}\to\Xi_c'^{0}) = -(\Xi_c^{*0+}\to\Omega_c^{0}),
\end{aligned}
\tag{36}
$$

the SU(3) symmetric relations

$$
\begin{aligned}
(\Sigma_c^{+}\to\Lambda_c^{+}) &= -2(\Xi_c'^{+}\to\Xi_c^{+}) = -(\Sigma_c^{++}\to\Xi_c^{+}) = \sqrt{2}(\Xi_c'^{0}\to\Lambda_c^{+}) = -(\Omega_c^{0}\to\Xi_c^{0})\\
(\Sigma_c^{*++}\to\Sigma_c^{++}) &= 2(\Xi_c^{*+}\to\Xi_c'^{+}) = (\Xi_c^{*+}\to\Sigma_c^{++}) = (\Omega_c^{*0}\to\Xi_c'^{+}),
\end{aligned}
\tag{37}
$$

and the various sum rules as follows

$$
\begin{aligned}
(\Sigma^{*+} \to \Sigma_c^{++}) &= (\Xi_c^{*+} \to \Omega_c^0) + (\Xi_c^{*+} \to \Sigma_c^{++}) - \sqrt{2}(\Xi_c^{*+} \to \Xi_c^{\prime 0}) \\
(\Sigma^{*+} \to \Xi_c^0) &= -\frac{1}{2}(\Xi_c^{\prime 0} \to \Lambda_c^+) + \frac{1}{\sqrt{2}}(\Xi_c^{*+} \to \Xi_c^+) + \frac{\sqrt{3}}{2\sqrt{2}}(\Xi_c^{\prime +} \to \Omega_c^0) \\
&\quad + \frac{1}{4\sqrt{6}}(\Xi_c^{*+} \to \Sigma_c^{++}) - \frac{5}{4\sqrt{3}}(\Xi_c^{*+} \to \Xi_c^{\prime 0}) \\
(\Sigma^{*+} \to \Lambda_c^+) &= \frac{3}{2\sqrt{2}}(\Xi_c^{\prime 0} \to \Lambda_c^+) - \frac{1}{2}(\Xi_c^{*+} \to \Xi_c^+) + \frac{3\sqrt{3}}{4}(\Xi_c^{\prime +} \to \Omega_c^0) \\
&\quad + \frac{\sqrt{3}}{8}(\Xi_c^{*+} \to \Sigma_c^{++}) - \frac{5\sqrt{3}}{4\sqrt{2}}(\Xi_c^{*+} \to \Xi_c^{\prime 0}) \\
(\Omega_c^{*0} \to \Xi_c^+) &= -\frac{1}{2\sqrt{2}}(\Xi_c^{\prime 0} \to \Lambda_c^+) + \frac{3}{2}(\Xi_c^{*+} \to \Xi_c^+) + \frac{3\sqrt{3}}{4}(\Xi_c^{\prime +} \to \Omega_c^0) \\
&\quad + \frac{\sqrt{3}}{8}(\Xi_c^{*+} \to \Sigma_c^{++}) - \frac{5\sqrt{3}}{4\sqrt{2}}(\Xi_c^{*+} \to \Xi_c^{\prime 0}). \qquad (38)
\end{aligned}
$$

These relations indicate that not all form factors are independent. As we will show soon, we will only have two different form factors, from which all other form factors can be easily obtained when flavor SU(3) symmetry is imposed.

While there are no experimental information on the axial-vector transition form factors of the singly heavy baryons, their strong decay widths are experimentally known. In particular, the Belle Collaboration has recently reported those for the $\Sigma_c^+ \to \Lambda_c^+ + \pi^0$ and $\Sigma_c^{*+} \to \Lambda_c^+ + \pi^0$ decays [55]. Thus, we will also compute all possible strong decay widths for the singly heavy baryons, using the following formulas

$$
\begin{aligned}
\Gamma_{B_{1/2} \to B_{1/2} m_\pi} &= \frac{1}{8\pi} \frac{|\boldsymbol{q}|^3}{f_\pi^2} \frac{M_f}{M_i} (G_{A,B \to B'}(0))^2, \\
\Gamma_{B_{3/2} \to B_{1/2} m_\pi} &= \frac{1}{12\pi} \frac{|\boldsymbol{q}|^3}{f_\pi^2} \frac{M_f}{M_i} (C^A_{5,B \to B'}(0))^2, \qquad (39)
\end{aligned}
$$

where the pion momentum $|\boldsymbol{q}|$ is given by

$$
|\boldsymbol{q}| = \frac{1}{2M_i} \sqrt{(M_i^2 - (M_f^2 + m_8)^2)(M_i^2 - (M_f^2 - m_8)^2)}. \qquad (40)
$$

M_i, M_f are the initial and final baryon masses, respectively. m_π represents the mass of the pion and f_π stands for the pion decay constant. The mass ratio M_f/M_i in Eq. (39) arises from the recoil effect [41,56]. Since the velocities of B_i and B_f are the same to order $\mathcal{O}(1/m_Q)$ in effective heavy quark theory, the recoil effects can be given by the mass ratio.

V. RESULTS AND DISCUSSION

We now show the results for the axial-vector transition form factors of the singly heavy baryons and discuss them. We first explain how the model parameters are fixed. In the χQSM, four different parameters need to be determined: the dynamical quark mass M, the cutoff mass Λ in the regularization functions, the strange current quark mass m_s, and the average of the up and down current quarks $\bar{m}$, as mentioned in Sec. III. $\bar{m}$ is determined by reproducing the physical value of the charged pion mass, $m_\pi = 140$ MeV. As explained in Refs. [50,57], The strange current quark mass is usually fixed by the kaon mass, $m_K = 495$ MeV and obtained to be around $m_s = 150$ MeV. However, we use $m_s = 180$ MeV, because it reproduces the mass spectra of the baryon octet and decuplet [50,57] very well. This value is larger than that in QCD [1] ($m_s = 93.4^{+8.6}_{-3.4}$ MeV). The present value of m_s should be taken to be an effective one. We consider the linear m_s corrections. Higher-order corrections may be included as done in Ref. [58] within the framework of the SU(3) Skyrme model. There is a caveat in dealing with these corrections. Since the current quark mass term in the effective chiral action give in Eq. (13) is introduced such that the low-energy theorems are satisfied. Note that this action is a model one. This means that the m_s^2-order term may be also included. However, there is no theoretical constraint to determine its form. Thus, the present scheme in dealing with the linear m_s corrections is a theoretically consistent. Moreover, as will be shown soon, the effects of the explicit SU(3) symmetry breaking are tiny. Thus, even though we take the value of m_s in QCD, the conclusion of the current work is not changed. The cutoff mass Λ is fixed by the pion decay constant $f_\pi = 93$ MeV. The dynamical quark mass M is regarded as a free parameter in the χQSM. Nevertheless, we use $M = 420$ MeV because one can produce various experimental data such as the radius of the proton [59], the magnetic dipole moments [60], and semileptonic decays of hyperons [61,62]. Note that the values of all the parameters are the same as in the previous works [28,33,34,51].

Since we use the $1/N_c$ and $1/m_Q$ expansion as a guiding principle, we have to maintain consistency in dealing with its expansion within the theoretical framework. So, we can ignore the mass difference in the momentum transfer. It indicates that momentum transfer in Eq. (4) can be approximated to be $\boldsymbol{q}^2 \approx -Q^2$. The expressions for $G_A^{(\chi)}$ and $C_5^{A(\chi)}$ contain the masses of the singly heavy baryons. Keeping the $1/N_c$ expansion in mind, we approximate M_i and M_f by $M_{\rm cl} + m_{\rm c}$. The baryon masses in the χQSM also include the rotational $1/N_c$ and $m_{\rm s}$ corrections. If we turn off all the corrections, the singly heavy baryon mass becomes the classical $N_c - 1$ soliton mass $M_{\rm cl}$ plus the charm quark mass. To be theoretically more consistent, hence, we will take $M_{\rm cl} + m_{\rm c}$ instead of a antitriplet and sextet baryon masses. In effect, the numerical results are improved by considering $M_{\rm cl} + m_{\rm c}$ in place of $M_{\bar{3}}$ and M_6 by around 10%. Similar approximations were performed in the case of the baryon octet and decuplet [51,63,64].

Concerning the $1/m_Q$ corrections, we need them only for the removal of degeneracy in the baryon sextet, as done in Ref. [17]. Since the charm quark mass is around 1.2 GeV, one may consider the $1/m_c$ corrections to other observables. Possible $1/m_c$ corrections to the isospin mass splittings of the singly heavy baryons were examined [30], they are negligibly small. So, we ignore the $1/m_Q$ corrections to the transition axial-vector form factors.

As shown in Eqs. (36) and (37), we have only two independent axial-vector transition form factors when the flavor SU(3) symmetry is considered. We will present the results for these two form factors. In left panel of Fig. 2, we draw the results for the axial-vector transition form factors for the $\Sigma_c^+ \to \Lambda_c^+$ transition. All other form factors for the axial-vector transitions $B_{1/2} \to B'_{1/2}$ are related to that for the $\Sigma_c^+ \to \Lambda_c^+$ transition. So, we take the $\Sigma_c^+ \to \Lambda_c^+$ transition form factor as a prototype one. The dashed curve represents that in the flavor SU(3) symmetric case, while the solid one depicts that with linear $m_{\rm s}$ corrections. The effects of SU(3) symmetry breaking are tiny. This can be understood by examining Eqs. (B1)–(B3). The prefactors in Eqs. (B2) and (B3) are much smaller than that in the leading-order contribution given in Eq. (B1). In addition, the first term in the bracket of Eq. (B1) is the most dominant one. In the right panel of Fig. 2, we depict the results for the axial-vector transition form factors from Σ_c^{*++} belonging to the baryon sextet with spin $3/2$ to Σ_c^{++} in the sextet with spin $1/2$. Note that the expression for the leading-order contribution to $C^A_{5,B\to B'}(Q^2)$ is distinguished from that for $G_{A,B\to B'}(Q^2)$ by the last term in Eq. (B4), which is proportional to $\mathcal{B}_0^{B\to B'}$ and $\mathcal{B}_2^{B\to B'}$. They provide about 9% corrections to $C^A_{5,B\to B'}(Q^2)$. The effects of the flavor SU(3) symmetry breaking turn out very small. Thus, we will neglect them in the discussion of other observables related to the axial-vector transition form factors.

It is of great interest to compare the Q^2 dependence of the result for $C^A_{5,\Sigma_c^{*++}\to\Sigma_c^{++}}(Q^2)$ to that for $C^A_{5,\Delta^+\to p}(Q^2)$, since both form factors describe the axial-vector transitions from the spin-$3/2$ baryon to the spin-$1/2$ baryon. To compare more closely, we normalize them by the corresponding values of the form factors at $Q^2 = 0$. As shown in Fig. 3, the axial-vector form factor for the $\Sigma_c^{*++} \to \Sigma_c^{++}$ transition starts to fall off more fast than that for the $\Delta^+ \to p$ transition. It indicates that the mean square radius for the $\Sigma_c^{*++} \to \Sigma_c^{++}$ transition is larger than that for the $\Delta^+ \to p$ one. We want to emphasize that the pion mean field for the singly heavy baryons is different from that for the light baryons. This makes main difference between the $\Sigma_c^{*++} \to \Sigma_c^{++}$ and $\Delta^+ \to p$ transition form factors, as exhibited in Fig. 3.

In Table I, we list the values of the $G_{A,\Sigma_c^+\to\Lambda_c^+}(0)$ and $C^A_{5,\Sigma_c^{*++}\to\Sigma_c^{++}}(0)$ at $Q^2 = 0$. These values will be used for determining the decay widths for the strong decays of the singly heavy baryons. The axial-vector transition form factor $G_{A,\Sigma_c^+\to\lambda_c^+}(Q^2)$ presented in Fig. 2 can be parametrized by the dipole-type parametrization

$$G_A = \frac{G_A(0)}{(1 + Q^2/M_A^2)^2}, \tag{41}$$

where M_A is called the axial mass. We can parametrize $C^A_{5,\Sigma_c^{*++}\to\Sigma_c^{++}}(Q^2)$ in the same manner. The numerical results for M_A are given in the third row in Table I, which indicates that the Q^2 dependence of the $\Sigma_c^+ \to \Lambda_c^+$ and $\Sigma_c^{*++} \to \Sigma_c^{++}$ form factors are similar. The results for the mean square radii are listed in the last row of Table I.

In Table II, we compare the current results for the strong decay widths of the singly heavy baryons, of which the experimental data are available. Thus, we consider the strong decays of Σ_c, Σ_c^*, and Ξ_c^*. The third column of Table II are the experimental data taken from the PDG [1]. In the fourth, fifth, and sixth columns of Table II, we list the experimental data taken from the FOCUS Collaboration [65], the CLEO Collaboration [66], and the Belle Collaboration [55,67,68], respectively. Though the current results for the strong decay of Σ_c seem overestimated, compared with the PDG data [1], they are very close to the CLEO II data [66]. On the other hand, the results for the Σ_c^* decay are larger than the experimental data. Note that the Σ_c^* baryon is a spin $3/2$ one and has a larger decay width than Σ_c. It reminds us of the strong decay of the Δ isobar. The result for the Δ strong decay from the χQSM is also deviated from the experimental data [69]. Since the Δ isobar appears as a resonance from πN scattering, the pion-loop corrections come into significant play. Similarly, they may contribute to the Σ_c^* decay. The results for the Ξ_c^* decays are in good agreement with the data. In Tables III and IV, we compare the current results with those from other works. We find that the results from the present work are consistent with those from Refs. [44,45].

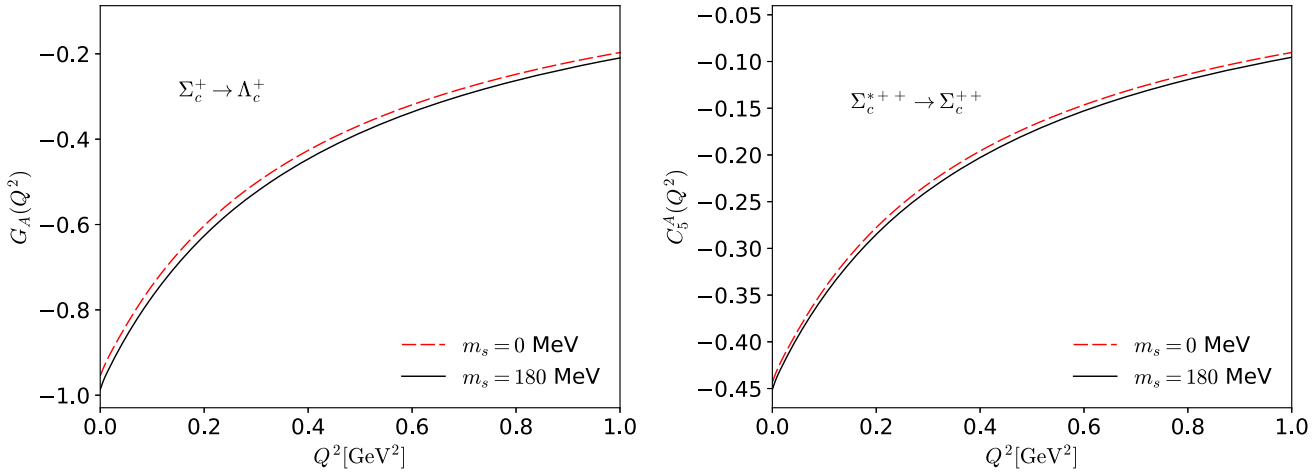

FIG. 2. The axial-vector transition form factor $G^{(3)}_{A,\Sigma_c^+\to\Lambda_c^+}(Q^2)$ $\left(C^{A(3)}_{5,\Sigma_c^{*++}\to\Sigma_c^{++}}(Q^2)\right)$ for the transitions from the baryon sextet with spin-1/2 (3/2) to the baryon antitriplet. In the left panel, the form factors for the $\Sigma_c^+ \to \Lambda_c^+$ transition are drawn, whereas in the right panel, those for the $\Sigma_c^{*++} \to \Sigma_c^{++}$ are depicted. The solid and dashed curves represent the total results with the effects of the flavor SU(3) symmetry breaking and those in the SU(3) symmetric case, respectively.

VI. SUMMARY AND CONCLUSION

We investigated the axial-vector transition form factors of the baryon sextet within the framework of the chiral quark-soliton model. Assuming that the heavy-quark mass is infinitely heavy, the $N_c - 1$ light valence quarks govern the quark dynamics inside a singly heavy baryon. In contrast, the singly heavy quark is merely a static color source, making singly heavy baryons the color singlet. The presence of the $N_c - 1$ valence quarks creates the pion mean field, so that they are also influenced by it self-consistently. The $N_c - 1$ valence quarks also constrain the right hypercharge $Y_R = (N_c - 1)/3 = 2/3$, allowing the flavor SU(3) representations such as the baryon antitriplet, baryon sextet, and higher representations. Based on this framework, we studied the axial-vector transitions from the baryon sextet with spin $1/2$ and $3/2$ to the baryon sextet with spin $1/2$ and antitriplet, considering the rotational $1/N_c$ and linear m_s corrections. We presented the results for the $\Sigma_c^+ \to \Lambda_c^+$ and $\Sigma_c^{*++} \to \Sigma_c^{++}$ form factors. These are the first results for the axial-vector transition form factors of the singly heavy baryons. Those for all other decay channels are related either by isospin symmetry or by flavor SU(3) symmetry. We found that the effects of the flavor SU(3) symmetry breaking were tiny. Thus, we neglected them to compute other observables. We also obtained the corresponding axial masses employing the dipole-type parametrizations for the form factors. We derived the axial-transition mean square radii. Using the values of the form factors at $Q^2 = 0$, we got the decay rates for the strong decays of Σ_c, Σ_c^*, and Ξ_c^*. The decay rates of Σ_c and Σ_c^* decays are overestimated in comparison with the data but those of the Ξ_c^* decays are in good agreement with the data.

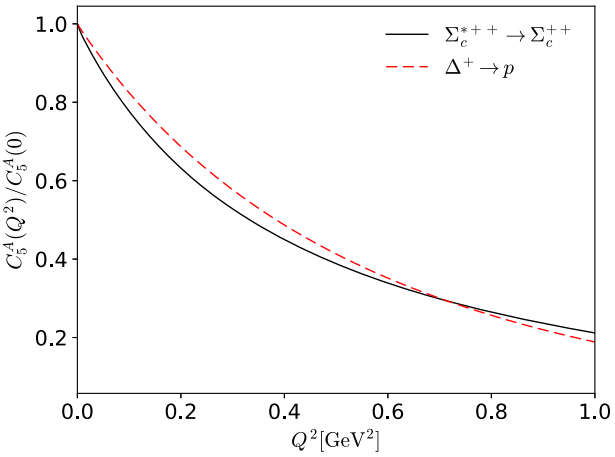

FIG. 3. Comparison of Q^2 dependence of $C^A_{5,\Sigma_c^{*++}\to\Sigma_c^{++}}(Q^2)$ to $C^A_{5,\Delta^+\to p}(Q^2)$. The solid curve represents the result for $C^A_{5,\Sigma_c^{*++}\to\Sigma_c^{++}}(Q^2)$, whereas the dashed one depicts $C^A_{5,\Delta^+\to p}(Q^2)$.

ACKNOWLEDGMENTS

The authors are grateful to Gh.-S. Yang and J.-Y. Kim for fruitful discussions. We also want to express our gratitude to Y.-S. Jun for his contribution to the initial stage of the current work. The present work was supported by an Inha University Research Grant in 2022.

TABLE I. Numerical results for the axial-vector transition constants $G_{A,\Sigma_c^+\to\Lambda_c^+}(0)(C^A_{5,\Sigma_c^{*++}\to\Sigma_c^{++}}(0))$, and the corresponding axial masses and mean square radii.

	$\Sigma_c^+ \to \Lambda_c^+$	$\Sigma_c^{*++} \to \Sigma_c^{++}$
$G_{A,\Sigma_c^+\to\Lambda_c^+}(0)(C^A_{5,\Sigma_c^{*++}\to\Sigma_c^{++}}(0))$	−0.955	−0.443
M_A [GeV]	0.759	0.728
$\langle r_A^2\rangle$ [fm^2]	0.812	0.882

TABLE II. Numerical results for the strong decay widths in comparison with the experimental data.

Decay modes	Γ (MeV)	Experimental data [1]	FOCUS Collaboration [65]	CLEO II experiment [66]	Belle experiment [55,67,68]
$\Sigma_c^{++} \to \Lambda_c^+ + \pi^+$	2.80	$1.89^{+0.09}_{-0.18}$	$2.05^{+0.41}_{-0.38}$	$2.3 \pm 0.2 \pm 0.3$	$1.84 \pm 0.04^{+0.07}_{-0.20}$
$\Sigma_c^{+} \to \Lambda_c^+ + \pi^0$	3.39	< 4.6	⋯	⋯	$2.3 \pm 0.3 \pm 0.3$
$\Sigma_c^{0} \to \Lambda_c^+ + \pi^-$	2.76	$1.83^{+0.11}_{-0.19}$	$1.55^{+0.41}_{-0.37}$	$2.5 \pm 0.2 \pm 0.3$	$1.76 \pm 0.04^{+0.09}_{-0.21}$
$\Sigma_c^{*++} \to \Lambda_c^+ + \pi^+$	21.0	$14.78^{+0.30}_{-0.40}$	⋯	⋯	$14.77 \pm 0.25^{+0.18}_{-0.30}$
$\Sigma_c^{*+} \to \Lambda_c^+ + \pi^0$	22.1	< 17	⋯	⋯	$17.2^{+2.3+3.1}_{-2.1-0.7}$
$\Sigma_c^{*0} \to \Lambda_c^+ + \pi^-$	21.0	$15.3^{+0.4}_{-0.5}$	⋯	⋯	$15.41 \pm 0.41^{+0.20}_{-0.32}$
$\Xi_c^{*+} \to \Xi_c + \pi$	2.12	2.14 ± 0.19	⋯	⋯	$2.6 \pm 0.2 \pm 0.4$
$\Xi_c^{*0} \to \Xi_c + \pi$	2.30	2.35 ± 0.22	⋯	⋯	⋯

TABLE III. Numerical results for the strong decay widths in comparison with those from various works.

Decay modes	Γ (MeV)	Yan *et al.* [38]	Huang *et al.* [39]	Rosner [42]	Pirjol *et al.* [40]	Tawfiq *et al.* [43]	Ivanov *et al.* [44]
$\Sigma_c^{++} \to \Lambda_c^+ + \pi^+$	2.80	⋯	2.5	1.32 ± 0.04	$2.025^{+1.134}_{-0.987}$	1.64	2.85 ± 0.19
$\Sigma_c^{+} \to \Lambda_c^+ + \pi^0$	3.39	⋯	3.2	1.32 ± 0.04	⋯	1.70	3.63 ± 0.27
$\Sigma_c^{0} \to \Lambda_c^+ + \pi^-$	2.76	2.45,4.35	2.4	1.32 ± 0.04	$1.939^{+1.114}_{-0.954}$	1.57	2.65 ± 0.19
$\Sigma_c^{*++} \to \Lambda_c^+ + \pi^+$	21.0	⋯	25	20	⋯	12.84	21.99 ± 0.87
$\Sigma_c^{*+} \to \Lambda_c^+ + \pi^0$	22.1	⋯	25	20	⋯	⋯	⋯
$\Sigma_c^{*0} \to \Lambda_c^+ + \pi^-$	21.0	⋯	25	20	⋯	12.40	21.21 ± 0.81
$\Xi_c^{*+} \to \Xi_c + \pi$	2.12	⋯	⋯	2.3 ± 0.1	⋯	1.12	1.78 ± 0.33
$\Xi_c^{*0} \to \Xi_c + \pi$	2.30	⋯	⋯	2.3 ± 0.1	⋯	1.16	2.11 ± 0.29

APPENDIX A: COMPONENTS OF THE AXIAL-VECTOR TRANSITION FORM FACTORS

In this appendix, the expressions for the axial-vector transition form factors in Eqs. (32) and (33) will be given explicitly

$$\mathcal{A}_0^{B\to B'}(Q^2) = \frac{\sqrt{M_{B'}}}{\sqrt{E_{B'}+M_{B'}}} \int d^3r j_0(|\boldsymbol{q}||\boldsymbol{r}|) \times \left[(N_c-1)\phi^\dagger_{\rm val}(\boldsymbol{r})\boldsymbol{\sigma}\cdot\boldsymbol{\tau}\phi_{\rm val}(r) + N_c \sum_n \phi_n^\dagger(\boldsymbol{r})\boldsymbol{\sigma}\cdot\boldsymbol{\tau}\phi_n(\boldsymbol{r})\mathcal{R}_1(E_n) \right], \quad \text{(A1)}$$

TABLE IV. Numerical results for the strong decay widths in comparison with those from various works.

Decay modes	Γ (MeV)	Albertus *et al.* [45]	Chen *et al.* [47]	Azizi *et al.* [48]	Cheng *et al.* [41]	Nagahiro *et al.* [46]	Can *et al.* [49]
$\Sigma_c^{++} \to \Lambda_c^+ + \pi^+$	2.80	$2.41 \pm 0.07 \pm 0.02$	1.24	2.16 ± 0.85	⋯	4.27–4.33	$1.65 \pm 0.28 \pm 0.30$
$\Sigma_c^{+} \to \Lambda_c^+ + \pi^0$	3.39	$2.79 \pm 0.08 \pm 0.02$	1.40	2.16 ± 0.85	$2.3^{+0.1}_{-0.2}$	⋯	$1.65 \pm 0.28 \pm 0.30$
$\Sigma_c^{0} \to \Lambda_c^+ + \pi^-$	2.76	$2.37 \pm 0.07 \pm 0.02$	1.24	2.16 ± 0.85	$1.9^{+0.1}_{-0.2}$	⋯	$1.65 \pm 0.28 \pm 0.30$
$\Sigma_c^{*++} \to \Lambda_c^+ + \pi^+$	21.0	$17.52 \pm 0.74 \pm 0.12$	11.9	⋯	$14.5^{+0.5}_{-0.8}$	30.3–31.6	⋯
$\Sigma_c^{*+} \to \Lambda_c^+ + \pi^0$	22.1	$17.31 \pm 0.73 \pm 0.12$	12.1	⋯	$15.2^{+0.6}_{-1.3}$	⋯	⋯
$\Sigma_c^{*0} \to \Lambda_c^+ + \pi^-$	21.0	$16.90 \pm 0.71 \pm 0.12$	11.9	⋯	$14.7^{+0.6}_{-1.2}$	⋯	⋯
$\Xi_c^{*+} \to \Xi_c + \pi$	2.12	$1.84 \pm 0.06 \pm 0.01$	0.64	⋯	$2.4^{+0.1}_{-0.2}$	⋯	⋯
$\Xi_c^{*0} \to \Xi_c + \pi$	2.30	$2.07 \pm 0.07 \pm 0.01$	0.54	⋯	$2.5^{+0.1}_{-0.2}$	⋯	⋯

$$\mathcal{B}_0^{B\to B'}(Q^2) = \frac{\sqrt{M_{B'}}}{\sqrt{E_{B'}+M_{B'}}}\int d^3r j_0(|\boldsymbol{q}||\boldsymbol{r}|)\Bigg[(N_c-1)\sum_{n\neq \mathrm{val}}\frac{1}{E_{\mathrm{val}}-E_n}\phi^\dagger_{\mathrm{val}}(\boldsymbol{r})\boldsymbol{\sigma}\phi_n(\boldsymbol{r})\cdot\langle n|\boldsymbol{\tau}|\mathrm{val}\rangle$$
$$-\frac{1}{2}N_c\sum_{n,m}\phi^\dagger_n(\boldsymbol{r})\boldsymbol{\sigma}\phi_m(\boldsymbol{r})\cdot\langle m|\boldsymbol{\tau}|n\rangle\mathcal{R}_5(E_n,E_m)\Bigg], \tag{A2}$$

$$\mathcal{C}_0^{B\to B'}(Q^2) = \frac{\sqrt{M_{B'}}}{\sqrt{E_{B'}+M_{B'}}}\int d^3r j_0(|\boldsymbol{q}||\boldsymbol{r}|)\Bigg[(N_c-1)\sum_{n_0\neq \mathrm{val}}\frac{1}{E_{\mathrm{val}}-E_{n_0}}\phi^\dagger_{\mathrm{val}}(\boldsymbol{r})\boldsymbol{\sigma}\cdot\boldsymbol{\tau}\phi_{n_0}(\boldsymbol{r})\langle n_0|\mathrm{val}\rangle$$
$$-N_c\sum_{n,m_0}\phi^\dagger_n(\boldsymbol{r})\boldsymbol{\sigma}\cdot\boldsymbol{\tau}\phi_{m_0}(\boldsymbol{r})\langle m_0|n\rangle\mathcal{R}_5(E_n,E_{m_0})\Bigg], \tag{A3}$$

$$\mathcal{D}_0^{B\to B'}(Q^2) = \frac{\sqrt{M_{B'}}}{\sqrt{E_{B'}+M_{B'}}}\int d^3r j_0(|\boldsymbol{q}||\boldsymbol{r}|)\Bigg[(N_c-1)\sum_{n\neq \mathrm{val}}\frac{\mathrm{sgn}(E_n)}{E_{\mathrm{val}}-E_n}\phi^\dagger_{\mathrm{val}}(\boldsymbol{r})(\boldsymbol{\sigma}\times\boldsymbol{\tau})\phi_n(\boldsymbol{r})\cdot\langle n|\boldsymbol{\tau}|\mathrm{val}\rangle$$
$$+\frac{1}{2}N_c\sum_{n,m}\phi^\dagger_n(\boldsymbol{r})\boldsymbol{\sigma}\times\boldsymbol{\tau}\phi_m(\boldsymbol{r})\cdot\langle m|\boldsymbol{\tau}|n\rangle\mathcal{R}_4(E_n,E_m)\Bigg], \tag{A4}$$

$$\mathcal{H}_0^{B\to B'}(Q^2) = \frac{\sqrt{M_{B'}}}{\sqrt{E_{B'}+M_{B'}}}\int d^3r j_0(|\boldsymbol{q}||\boldsymbol{r}|)\Bigg[(N_c-1)\sum_{n\neq \mathrm{val}}\frac{1}{E_{\mathrm{val}}-E_n}\phi^\dagger_{\mathrm{val}}(\boldsymbol{r})\boldsymbol{\sigma}\cdot\boldsymbol{\tau}\langle\boldsymbol{r}|n\rangle\langle n|\gamma^0|\mathrm{val}\rangle$$
$$+\frac{1}{2}N_c\sum_{n,m}\phi^\dagger_n(\boldsymbol{r})\boldsymbol{\sigma}\cdot\boldsymbol{\tau}\phi_m(\boldsymbol{r})\langle m|\gamma^0|n\rangle\mathcal{R}_2(E_n,E_m)\Bigg], \tag{A5}$$

$$\mathcal{I}_0^{B\to B'}(Q^2) = \frac{\sqrt{M_{B'}}}{\sqrt{E_{B'}+M_{B'}}}\int d^3r j_0(|\boldsymbol{q}||\boldsymbol{r}|)\Bigg[(N_c-1)\sum_{n\neq \mathrm{val}}\frac{1}{E_{\mathrm{val}}-E_n}\phi^\dagger_{\mathrm{val}}(\boldsymbol{r})\boldsymbol{\sigma}\phi_n(\boldsymbol{r})\cdot\langle n|\gamma^0\boldsymbol{\tau}|\mathrm{val}\rangle$$
$$+\frac{1}{2}N_c\sum_{n,m}\phi^\dagger_n(\boldsymbol{r})\boldsymbol{\sigma}\phi_m(\boldsymbol{r})\cdot\langle m|\gamma^0\boldsymbol{\tau}|n\rangle\mathcal{R}_2(E_n,E_m)\Bigg], \tag{A6}$$

$$\mathcal{J}_0^{B\to B'}(Q^2) = \frac{\sqrt{M_{B'}}}{\sqrt{E_{B'}+M_{B'}}}\int d^3r j_0(|\boldsymbol{q}||\boldsymbol{r}|)\Bigg[(N_c-1)\sum_{n_0\neq \mathrm{val}}\frac{1}{E_{\mathrm{val}}-E_{n_0}}\phi^\dagger_{\mathrm{val}}(\boldsymbol{r})\boldsymbol{\sigma}\cdot\boldsymbol{\tau}\phi_{n_0}(\boldsymbol{r})\langle n_0|\gamma^0|\mathrm{val}\rangle$$
$$+N_c\sum_{n,m_0}\phi^\dagger_n(\boldsymbol{r})\boldsymbol{\sigma}\cdot\boldsymbol{\tau}\phi_{m_0}(\boldsymbol{r})\langle m_0|\gamma^0|n\rangle\mathcal{R}_2(E_n,E_{m_0})\Bigg], \tag{A7}$$

$$\mathcal{A}_2^{B\to B'}(Q^2) = \frac{\sqrt{M_{B'}}}{\sqrt{E_{B'}+M_{B'}}}\int d^3r j_2(|\boldsymbol{q}||\boldsymbol{r}|)\Bigg[(N_c-1)\phi^\dagger_{\mathrm{val}}(\boldsymbol{r})\{\sqrt{2\pi}Y_2\otimes\sigma_1\}_1\cdot\boldsymbol{\tau}\phi_{\mathrm{val}}(\boldsymbol{r})$$
$$+N_c\sum_n\phi^\dagger_n(\boldsymbol{r})\{\sqrt{2\pi}Y_2\otimes\sigma_1\}_1\cdot\boldsymbol{\tau}\phi_n(\boldsymbol{r})\mathcal{R}_1(E_n)\Bigg], \tag{A8}$$

$$\mathcal{B}_2^{B\to B'}(Q^2) = \frac{\sqrt{M_{B'}}}{\sqrt{E_{B'}+M_{B'}}}\int d^3r j_2(|\boldsymbol{q}||\boldsymbol{r}|)\Bigg[(N_c-1)\sum_{n\neq \mathrm{val}}\frac{\langle n|\boldsymbol{\tau}|\mathrm{val}\rangle}{E_{\mathrm{val}}-E_n}\cdot\phi^\dagger_{\mathrm{val}}(\boldsymbol{r})\{\sqrt{2\pi}Y_2\otimes\sigma_1\}_1\phi_n(\boldsymbol{r})$$
$$-\frac{1}{2}N_c\sum_{n,m}\phi^\dagger_n(\boldsymbol{r})\{\sqrt{2\pi}Y_2\otimes\sigma_1\}_1\phi_m(\boldsymbol{r})\cdot\langle m|\boldsymbol{\tau}|n\rangle\mathcal{R}_5(E_n,E_m)\Bigg], \tag{A9}$$

$$\mathcal{C}_2^{B\to B'}(Q^2) = \frac{\sqrt{M_{B'}}}{\sqrt{E_{B'}+M_{B'}}}\int d^3r j_2(|\boldsymbol{q}||\boldsymbol{r}|)\Bigg[(N_c-1)\sum_{n_0\neq \mathrm{val}}\frac{\langle n_0|\mathrm{val}\rangle}{E_{\mathrm{val}}-E_{n_0}}\phi^\dagger_{\mathrm{val}}(\boldsymbol{r})\{\sqrt{2\pi}Y_2\otimes\sigma_1\}_1\cdot\boldsymbol{\tau}\phi_{n_0}(\boldsymbol{r})$$
$$-N_c\sum_{n,m_0}\phi^\dagger_n(\boldsymbol{r})\{\sqrt{2\pi}Y_2\otimes\sigma_1\}_1\cdot\boldsymbol{\tau}\phi_{m_0}(\boldsymbol{r})\langle m_0|n\rangle\mathcal{R}_5(E_n,E_{m_0})\Bigg], \tag{A10}$$

$$\mathcal{D}_2^{B\to B'}(Q^2)=\frac{\sqrt{M_{B'}}}{\sqrt{E_{B'}+M_{B'}}}\int d^3r j_2(|\boldsymbol{q}||\boldsymbol{r}|)\Bigg[(N_c-1)\sum_{n\neq\mathrm{val}}\frac{\mathrm{sgn}(E_n)\langle n|\boldsymbol{\tau}|\mathrm{val}\rangle}{E_{\mathrm{val}}-E_n}\cdot\phi^\dagger_{\mathrm{val}}(\boldsymbol{r})\{\sqrt{2\pi}Y_2\otimes\sigma_1\}_1\times\boldsymbol{\tau}\phi_n(\boldsymbol{r})$$
$$+\frac{1}{2}N_c\sum_{n,m}\phi^\dagger_n(\boldsymbol{r})\{\sqrt{2\pi}Y_2\otimes\sigma_1\}_1\times\boldsymbol{\tau}\phi_m(\boldsymbol{r})\cdot\langle m|\boldsymbol{\tau}|n\rangle\mathcal{R}_4(E_n,E_m)\Bigg], \tag{A11}$$

$$\mathcal{H}_2^{B\to B'}(Q^2)=\frac{\sqrt{M_{B'}}}{\sqrt{E_{B'}+M_{B'}}}\int d^3r j_2(|\boldsymbol{q}||\boldsymbol{r}|)\Bigg[(N_c-1)\sum_{n\neq\mathrm{val}}\frac{\langle n|\gamma^0|\mathrm{val}\rangle}{E_{\mathrm{val}}-E_n}\phi^\dagger_{\mathrm{val}}(\boldsymbol{r})\{\sqrt{2\pi}Y_2\otimes\sigma_1\}_1\cdot\boldsymbol{\tau}\phi_n(\boldsymbol{r})$$
$$+\frac{1}{2}N_c\sum_{n,m}\phi^\dagger_n(\boldsymbol{r})\{\sqrt{2\pi}Y_2\otimes\sigma_1\}_1\cdot\boldsymbol{\tau}\phi_m(\boldsymbol{r})\langle m|\gamma^0|n\rangle\mathcal{R}_2(E_n,E_m)\Bigg], \tag{A12}$$

$$\mathcal{I}_2^{B\to B'}(Q^2)=\frac{\sqrt{M_{B'}}}{\sqrt{E_{B'}+M_{B'}}}\int d^3r j_2(|\boldsymbol{q}||\boldsymbol{r}|)\Bigg[(N_c-1)\sum_{n\neq\mathrm{val}}\frac{\langle n|\gamma^0\boldsymbol{\tau}|\mathrm{val}\rangle}{E_{\mathrm{val}}-E_n}\cdot\phi^\dagger_{\mathrm{val}}(\boldsymbol{r})\{\sqrt{2\pi}Y_2\otimes\sigma_1\}_1\phi_n(\boldsymbol{r})$$
$$+\frac{1}{2}N_c\sum_{n,m}\phi^\dagger_n(\boldsymbol{r})\{\sqrt{2\pi}Y_2\otimes\sigma_1\}_1\phi_m(\boldsymbol{r})\cdot\langle m|\gamma^0\boldsymbol{\tau}|n\rangle\mathcal{R}_2(E_n,E_m)\Bigg], \tag{A13}$$

$$\mathcal{J}_2^{B\to B'}(Q^2)=\frac{\sqrt{M_{B'}}}{\sqrt{E_{B'}+M_{B'}}}\int d^3r j_2(|\boldsymbol{q}||\boldsymbol{r}|)\Bigg[(N_c-1)\sum_{n_0\neq\mathrm{val}}\frac{\langle n_0|\gamma^0|\mathrm{val}\rangle}{E_{\mathrm{val}}-E_{n_0}}\phi^\dagger_{\mathrm{val}}(\boldsymbol{r})\{\sqrt{2\pi}Y_2\otimes\sigma_1\}_1\cdot\boldsymbol{\tau}\phi_{n_0}(\boldsymbol{r})$$
$$+N_c\sum_{n,m_0}\phi^\dagger_n(\boldsymbol{r})\{\sqrt{2\pi}Y_2\otimes\sigma_1\}_1\cdot\boldsymbol{\tau}\phi_{m_0}(\boldsymbol{r})\langle m_0|\gamma^0|n\rangle\mathcal{R}_2(E_n,E_{m_0})\Bigg], \tag{A14}$$

where the regularization functions are defined by

$$\mathcal{R}_1(E_n)=\frac{-E_n}{2\sqrt{\pi}}\int_0^\infty\phi(u)\frac{du}{\sqrt{u}}e^{-uE_n^2}, \tag{A15}$$

$$\mathcal{R}_2(E_n,E_m)=\frac{1}{2\sqrt{\pi}}\int_0^\infty\phi(u)\frac{du}{\sqrt{u}}\frac{E_me^{-uE_m^2}-E_ne^{-uE_n^2}}{E_n-E_m}, \tag{A16}$$

$$\mathcal{R}_4(E_n,E_m)=\frac{1}{2\pi}\int_0^\infty du\phi(u)\int_0^1 d\alpha e^{-\alpha uE_m^2-(1-\alpha)uE_n^2}\frac{(1-\alpha)E_n-\alpha E_m}{\sqrt{\alpha(1-\alpha)}}, \tag{A17}$$

$$\mathcal{R}_5(E_n,E_m)=\frac{\mathrm{sgn}(E_n)-\mathrm{sgn}(E_m)}{2(E_n-E_m)}. \tag{A18}$$

Here, $|\mathrm{val}\rangle$ and $|n\rangle$ represent the state of the valence and sea quarks with the corresponding eigenenergies E_{val} and E_n of the one-body Dirac Hamiltonian $h(U)$, respectively.

APPENDIX B: DETAILED EXPRESSIONS FOR THE TRANSITION AXIAL-VECTOR FORM FACTORS

Having computed the transition matrix elements of the D functions in Eqs. (32) and (33), we obtain the following results respectively for $G^{(\chi)}_{A,B\to B'}(Q^2)^{(\mathrm{sym})}$, and $G^{(\chi)}_{A,B\to B'}(Q^2)^{(\mathrm{op})}$, and $G^{(\chi)}_{A,B\to B'}(Q^2)^{(\mathrm{wf})}$

$$G^{(\chi)}_{A,B\to B'}(Q^2)^{(\mathrm{sym})}=-\frac{\sqrt{3}}{36}\begin{pmatrix}\sqrt{2}\\ -\sqrt{2}T_3\\ -\sqrt{2}\\ 1\\ -\sqrt{2}\end{pmatrix}\Bigg[\Bigg\{2\{\mathcal{A}_0^{B\to B'}(Q^2)-\mathcal{A}_2^{B\to B'}(Q^2)\}-\frac{i\{\mathcal{D}_0^{B\to B'}(Q^2)-\mathcal{D}_2^{B\to B'}(Q^2)\}}{I_1}\Bigg\}$$
$$-\frac{\{\mathcal{C}_0^{B\to B'}(Q^2)-\mathcal{C}_2^{B\to B'}(Q^2)\}}{I_2}\Bigg], \tag{B1}$$

$$G^{(\chi)}_{A,B\to B'}(Q^2)^{(\mathrm{op})} = -\frac{\sqrt{3}m_s}{540}\left[\sqrt{2}\begin{pmatrix}\sqrt{2}\\ -2\sqrt{2}T_3\\ \sqrt{2}\\ -3\\ 0\end{pmatrix}\left\{\frac{K_1}{I_1}\{\mathcal{B}_0^{B\to B'}(Q^2)-\mathcal{B}_2^{B\to B'}(Q^2)\}-\{\mathcal{I}_0^{B\to B'}(Q^2)-\mathcal{I}_2^{B\to B'}(Q^2)\}\right\}\right.$$
$$+3\sqrt{2}\begin{pmatrix}2\sqrt{2}\\ -2\sqrt{2}T_3\\ -\sqrt{2}\\ 1\\ -\sqrt{2}\end{pmatrix}\left\{\frac{K_2}{I_2}\{\mathcal{C}_0^{B\to B'}(Q^2)-\mathcal{C}_2^{B\to B'}(Q^2)\}-\{\mathcal{J}_0^{B\to B'}(Q^2)-\mathcal{J}_2^{B\to B'}(Q^2)\}\right\}$$
$$\left.+\begin{pmatrix}7\sqrt{2}\\ -10\sqrt{2}T_3\\ -11\sqrt{2}\\ 9\\ -12\sqrt{2}\end{pmatrix}\{\mathcal{H}_0^{B\to B'}(Q^2)-\mathcal{H}_2^{B\to B'}(Q^2)\}\right], \tag{B2}$$

$$G^{(\chi)}_{A,B\to B'}(Q^2)^{(\mathrm{wf})} = -\frac{\sqrt{2}}{1440}p_{\overline{15}}\begin{pmatrix}2\\ -5T_3\\ -1\\ -3\sqrt{2}\\ 3\end{pmatrix}\left[\sqrt{2}\left\{2\{\mathcal{A}_0^{B\to B'}(Q^2)-\mathcal{A}_2^{B\to B'}(Q^2)\}-\frac{i\{\mathcal{D}_0^{B\to B'}(Q^2)-\mathcal{D}_2^{B\to B'}(Q^2)\}}{I_1}\right\}\right.$$
$$\left.+3\,\frac{\{\mathcal{C}_0^{B\to B'}(Q^2)-\mathcal{C}_2^{B\to B'}(Q^2)\}}{I_2}\right]$$
$$-\frac{\sqrt{30}}{7200}q_{\overline{15}}\left[\begin{pmatrix}4\\ -T_3\\ 8\\ -3\sqrt{2}\\ 0\end{pmatrix}\left\{2\{\mathcal{A}_0^{B\to B'}(Q^2)-\mathcal{A}_2^{B\to B'}(Q^2)\}-\frac{i\{\mathcal{D}_0^{B\to B'}(Q^2)-\mathcal{D}_2^{B\to B'}(Q^2)\}}{I_1}\right\}\right.$$
$$\left.-2\sqrt{5}\begin{pmatrix}4\sqrt{2}\\ -\sqrt{2}T_3\\ 4\sqrt{2}\\ -3\\ 0\end{pmatrix}\frac{\{\mathcal{C}_0^{B\to B'}(Q^2)-\mathcal{C}_2^{B\to B'}(Q^2)\}}{I_2}\right], \tag{B3}$$

in the basis of $[\Sigma_c^+\to\Lambda_c^+,\Xi_c'\to\Xi_c,\Sigma_c^{++}\to\Xi_c^+,\Xi_c'^0\to\Lambda_c^+,\Omega_c^0\to\Xi_c^0]$, and respectively for $C^{\mathcal{A}(\chi)}_{5,B\to B'}(Q^2)^{(\mathrm{sym})}$, $C^{\mathcal{A}(\chi)}_{5,B\to B'}(Q^2)^{(\mathrm{op})}$, and $C^{\mathcal{A}(\chi)}_{5,B\to B'}(Q^2)^{(\mathrm{wf})}$

$$C^{A(\chi)}_{5,B\to B'}(Q^2)^{(\mathrm{sym})} = -\frac{1}{90}\begin{pmatrix} T_3 \\ T_3 \\ 1 \\ 1 \end{pmatrix}\left[3\left\{2\{\mathcal{A}_0^{B\to B'}(Q^2) - \mathcal{A}_2^{B\to B'}(Q^2)\} - \frac{i\{\mathcal{D}_0^{B\to B'}(Q^2) - \mathcal{D}_2^{B\to B'}(Q^2)\}}{I_1}\right\}\right.$$
$$\left. - 3\frac{\{\mathcal{C}_0^{B\to B'}(Q^2) - \mathcal{C}_2^{B\to B'}(Q^2)\}}{I_2} - 2\frac{\{\mathcal{B}_0^{B\to B'}(Q^2) - \mathcal{B}_2^{B\to B'}(Q^2)\}}{I_1}\right], \tag{B4}$$

$$C^{A(\chi)}_{5,B\to B'}(Q^2)^{(\mathrm{op})} = -\frac{2\sqrt{2}m_s}{810}\left[\sqrt{2}\begin{pmatrix} 4T_3 \\ T_3 \\ -1 \\ -3 \end{pmatrix}\left\{\frac{K_1}{I_1}\{\mathcal{B}_0^{B\to B'}(Q^2) - \mathcal{B}_2^{B\to B'}(Q^2)\} - \{\mathcal{I}_0^{B\to B'}(Q^2) - \mathcal{I}_2^{B\to B'}(Q^2)\}\right\}\right.$$
$$+\sqrt{2}\begin{pmatrix} 10T_3 \\ 14T_3 \\ -7 \\ -3 \end{pmatrix}\left\{\frac{K_2}{I_2}\{\mathcal{C}_0^{B\to B'}(Q^2) - \mathcal{C}_2^{B\to B'}(Q^2)\} - \{\mathcal{J}_0^{B\to B'}(Q^2) - \mathcal{J}_2^{B\to B'}(Q^2)\}\right\}$$
$$\left.+\begin{pmatrix} 14\sqrt{2}T_3 \\ 16\sqrt{2}T_3 \\ 19\sqrt{2} \\ 21 \end{pmatrix}\{\mathcal{H}_0^{B\to B'}(Q^2) - \mathcal{H}_2^{B\to B'}(Q^2)\}\right], \tag{B5}$$

$$C^{A(\chi)}_{5,B\to B'}(Q^2)^{(\mathrm{wf})} = -\frac{1}{90}q_{\overline{15}}\left[2\sqrt{5}\begin{pmatrix} 8T_3 \\ 4T_3 \\ -5 \\ -3 \end{pmatrix}\left\{2\{\mathcal{A}_0^{B\to B'}(Q^2) - \mathcal{A}_2^{B\to B'}(Q^2)\} - \frac{i\{\mathcal{D}_0^{B\to B'}(Q^2) - \mathcal{D}_2^{B\to B'}(Q^2)\}}{I_1}\right\}\right.$$
$$+\sqrt{5}\begin{pmatrix} 8T_3 \\ 5T_3 \\ -5 \\ 3 \end{pmatrix}\frac{\{\mathcal{C}_0^{B\to B'}(Q^2) - \mathcal{C}_2^{B\to B'}(Q^2)\}}{I_2} - 2\begin{pmatrix} 6\sqrt{6}T_3 \\ 15T_3 \\ 5\sqrt{15} \\ 3\sqrt{15} \end{pmatrix}\frac{\{\mathcal{B}_0^{B\to B'}(Q^2) - \mathcal{B}_2^{B\to B'}(Q^2)\}}{I_1}\Bigg]$$
$$+\frac{\sqrt{5}}{5400}q_{\overline{24}}\left[\sqrt{2}\begin{pmatrix} 0 \\ 0 \\ 2 \\ -1 \end{pmatrix}\left\{2\{\mathcal{A}_0^{B\to B'}(Q^2) - \mathcal{A}_2^{B\to B'}(Q^2)\} - \frac{i\{\mathcal{D}_0^{B\to B'}(Q^2) - \mathcal{D}_2^{B\to B'}(Q^2)\}}{I_1}\right\}\right.$$
$$\left.+8\sqrt{2}\begin{pmatrix} 0 \\ 0 \\ 1 \\ 0 \end{pmatrix}\frac{\{\mathcal{C}_0^{B\to B'}(Q^2) - \mathcal{C}_2^{B\to B'}(Q^2)\}}{I_2} + 40\begin{pmatrix} 0 \\ 0 \\ 1 \\ 0 \end{pmatrix}\frac{\{\mathcal{B}_0^{B\to B'}(Q^2) - \mathcal{B}_2^{B\to B'}(Q^2)\}}{I_1}\right] \tag{B6}$$

in the basis of $[\Sigma_c^* \to \Sigma_c, \Xi_c^* \to \Xi_c', \Xi_c^{*+} \to \Sigma_c^{++}, \Omega_c^{*0} \to \Xi_c'^{+}]$. The explicit expressions for $\mathcal{A}_i^{B\to B'}$, $\mathcal{B}_i^{B\to B'}$, $\mathcal{C}_i^{B\to B'}$, $\mathcal{D}_i^{B\to B'}$, $\mathcal{I}_i^{B\to B'}$, $\mathcal{J}_i^{B\to B'}$, and $\mathcal{H}_i^{B\to B'}$ can be found in Appendix A. The matrix elements of the collective operators are given in Appendix C in detail.

APPENDIX C: MATRIX ELEMENTS OF THE SU(3) WIGNER D FUNCTION

In the following we list the results for the matrix elements of the relevant collective operators for the axial-vector transition form factors of the singly heavy baryons in Tables V–XII.

TABLE V. The matrix elements of the single and double Wigner D function operators when $a = 3$.

$B \to B'$	$\Sigma_c^+ \to \Lambda_c^+$	$\Xi_c' \to \Xi_c$	$\Sigma_c^{*+} \to \Lambda_c^+$	$\Xi_c^* \to \Xi_c$	$\Sigma_c^* \to \Sigma_c$	$\Xi_c^* \to \Xi_c'$	$\Omega_c^{*0} \to \Omega_c^0$
$\langle B'\vert D_{33}^{(8)}\vert B\rangle$	$-\frac{1}{2\sqrt{6}}$	$\frac{1}{2\sqrt{6}}T_3$	$\frac{1}{2\sqrt{3}}$	$-\frac{1}{2\sqrt{3}}T_3$	$-\frac{1}{5\sqrt{2}}T_3$	$-\frac{1}{5\sqrt{2}}T_3$	0
$\langle B'\vert D_{38}^{(8)}\hat{J}_3\vert B\rangle$	0	0	0	0	$\frac{1}{5\sqrt{6}}T_3$	$\frac{1}{5\sqrt{6}}T_3$	0
$\langle B'\vert d_{bc3}D_{3b}^{(8)}\hat{J}_c\vert B\rangle$	$\frac{1}{4\sqrt{6}}$	$-\frac{1}{4\sqrt{6}}T_3$	$-\frac{1}{4\sqrt{3}}$	$\frac{1}{4\sqrt{3}}T_3$	$\frac{1}{10\sqrt{2}}T_3$	$\frac{1}{10\sqrt{2}}T_3$	0
$\langle B'\vert D_{83}^{(8)}D_{38}^{(8)}\vert B\rangle$	$-\frac{1}{20\sqrt{6}}$	$\frac{1}{5\sqrt{6}}T_3$	$\frac{1}{20\sqrt{3}}$	$-\frac{1}{5\sqrt{3}}T_3$	$-\frac{\sqrt{2}}{45}T_3$	$-\frac{1}{45\sqrt{2}}T_3$	0
$\langle B'\vert D_{88}^{(8)}D_{33}^{(8)}\vert B\rangle$	$-\frac{\sqrt{6}}{40}$	0	$\frac{\sqrt{3}}{20}$	0	$-\frac{\sqrt{2}}{45}T_3$	$-\frac{1}{45\sqrt{2}}T_3$	0
$\langle B'\vert d_{bc3}D_{8c}^{(8)}D_{3b}^{(8)}\vert B\rangle$	$-\frac{1}{10\sqrt{2}}$	$\frac{1}{10\sqrt{2}}T_3$	$\frac{1}{10}$	$-\frac{1}{10}T_3$	$-\frac{1}{9\sqrt{6}}T_3$	$-\frac{7}{45\sqrt{6}}T_3$	0

TABLE VI. The transition matrix elements of the single Wigner D function operators coming from the $\overline{15}$-plet component of the baryon wave functions when $a = 3$.

$B \to B'$	$\Sigma_c^+ \to \Lambda_c^+$	$\Xi_c' \to \Xi_c$	$\Sigma_c^{*+} \to \Lambda_c^+$	$\Xi_c^* \to \Xi_c$	$\Sigma_c^* \to \Sigma_c$	$\Xi_c^* \to \Xi_c'$	$\Omega_c^{*0} \to \Omega_c^0$
$\langle B'_{\overline{\mathbf{15}}}\vert D_{33}^{(8)}\vert B\rangle$	$-\frac{1}{6\sqrt{30}}$	$\frac{\sqrt{10}}{36}T_3$	$\frac{1}{6\sqrt{15}}$	$-\frac{\sqrt{5}}{18}T_3$	$-\frac{1}{9\sqrt{5}}T_3$	$-\frac{5}{9\sqrt{30}}T_3$	0
$\langle B'_{\overline{\mathbf{15}}}\vert D_{38}^{(8)}J_3\vert B\rangle$	0	0	0	0	$-\frac{1}{3\sqrt{15}}T_3$	$-\frac{5}{9\sqrt{10}}T_3$	0
$\langle B'_{\overline{\mathbf{15}}}\vert d_{ab3}D_{3a}^{(8)}J_b\vert B\rangle$	$-\frac{1}{4\sqrt{30}}$	$\frac{\sqrt{10}}{24}T_3$	$\frac{1}{4\sqrt{15}}$	$-\frac{\sqrt{5}}{12}T_3$	$-\frac{1}{18\sqrt{5}}T_3$	$-\frac{5}{18\sqrt{30}}T_3$	0
$\langle B'\vert D_{33}^{(8)}\vert B_{\overline{\mathbf{15}}}\rangle$	$-\frac{1}{2\sqrt{15}}$	$\frac{1}{6\sqrt{10}}T_3$	$\frac{1}{\sqrt{30}}$	$-\frac{1}{6\sqrt{5}}T_3$	$-\frac{1}{9\sqrt{5}}T_3$	$-\frac{5}{9\sqrt{30}}T_3$	0
$\langle B'\vert D_{38}^{(8)}J_3\vert B_{\overline{\mathbf{15}}}\rangle$	0	0	0	0	$-\frac{1}{3\sqrt{15}}T_3$	$-\frac{5}{9\sqrt{10}}T_3$	0
$\langle B'\vert d_{ab3}D_{3a}^{(8)}J_b\vert B_{\overline{\mathbf{15}}}\rangle$	$-\frac{1}{4\sqrt{15}}$	$\frac{1}{12\sqrt{10}}T_3$	$\frac{1}{2\sqrt{30}}$	$-\frac{1}{12\sqrt{5}}T_3$	$-\frac{1}{18\sqrt{5}}T_3$	$-\frac{5}{18\sqrt{30}}T_3$	0

TABLE VII. The transition matrix elements of the single Wigner D function operators coming from the $\overline{24}$-plet component of the baryon wave functions when $a = 3$.

$B \to B'$	$\Sigma_c^* \to \Sigma_c$	$\Xi_c^* \to \Xi_c'$	$\Omega_c^{*0} \to \Omega_c^0$
$\langle B'_{\overline{\mathbf{24}}}\vert D_{33}^{(8)}\vert B\rangle$	$-\frac{1}{90\sqrt{2}}T_3$	$-\frac{1}{45\sqrt{3}}T_3$	0
$\langle B'_{\overline{\mathbf{24}}}\vert D_{38}^{(8)}J_3\vert B\rangle$	$\frac{1}{15\sqrt{6}}T_3$	$\frac{2}{45}T_3$	0
$\langle B'_{\overline{\mathbf{24}}}\vert d_{ab3}D_{3a}^{(8)}J_b\vert B\rangle$	$-\frac{1}{45\sqrt{2}}T_3$	$-\frac{2}{45\sqrt{3}}T_3$	0
$\langle B'\vert D_{33}^{(8)}\vert B_{\overline{\mathbf{24}}}\rangle$	$-\frac{1}{90\sqrt{2}}T_3$	$-\frac{1}{45\sqrt{3}}T_3$	0
$\langle B'\vert D_{38}^{(8)}J_3\vert B_{\overline{\mathbf{24}}}\rangle$	$\frac{1}{15\sqrt{6}}T_3$	$\frac{2}{45}T_3$	0
$\langle B'\vert d_{ab3}D_{3a}^{(8)}J_b\vert B_{\overline{\mathbf{24}}}\rangle$	$-\frac{1}{45\sqrt{2}}T_3$	$-\frac{2}{45\sqrt{3}}T_3$	0

TABLE VIII. The matrix elements of the single and double Wigner D function operators when $a = 4 + i5$.

$B \to B'$	$\Sigma_c^{++} \to \Xi_c^+$	$\Sigma_c^{*++} \to \Xi_c^+$
$\langle B_{\bar{\mathbf{3}}}\|D^{(8)}_{p3}\|B_{\mathbf{6}}\rangle$	$\frac{1}{2\sqrt{6}}$	$-\frac{1}{2\sqrt{3}}$
$\langle B_{\bar{\mathbf{3}}}\|D^{(8)}_{p8}\hat{J}_3\|B_{\mathbf{6}}\rangle$	0	0
$\langle B_{\bar{\mathbf{3}}}\|d_{bc3}D^{(8)}_{pb}\hat{J}_c\|B_{\mathbf{6}}\rangle$	$-\frac{1}{4\sqrt{6}}$	$\frac{1}{4\sqrt{3}}$
$\langle B_{\bar{\mathbf{3}}}\|D^{(8)}_{83}D^{(8)}_{p8}\|B_{\mathbf{6}}\rangle$	$-\frac{1}{20\sqrt{6}}$	$\frac{1}{20\sqrt{3}}$
$\langle B_{\bar{\mathbf{3}}}\|D^{(8)}_{88}D^{(8)}_{p3}\|B_{\mathbf{6}}\rangle$	$-\frac{1}{20\sqrt{6}}$	$\frac{1}{20\sqrt{3}}$
$\langle B_{\bar{\mathbf{3}}}\|d_{bc3}D^{(8)}_{8c}D^{(8)}_{pb}\|B_{\mathbf{10}}\rangle$	$-\frac{1}{20\sqrt{2}}$	$\frac{1}{20}$

TABLE IX. The transition matrix elements of the single Wigner D function operators coming from the $\overline{15}$-plet component of the baryon wave functions when $a = 4 + i5$.

$B \to B'$	$\Sigma_c^{++} \to \Xi_c^+$	$\Sigma_c^{*++} \to \Xi_c^+$
$\langle B'_{\overline{\mathbf{15}}}\|D^{(8)}_{p3}\|B\rangle$	$\frac{1}{18\sqrt{10}}$	$-\frac{1}{18\sqrt{5}}$
$\langle B'_{\overline{\mathbf{15}}}\|D^{(8)}_{p8}J_3\|B\rangle$	0	0
$\langle B'_{\overline{\mathbf{15}}}\|d_{ab3}D^{(8)}_{pa}J_b\|B\rangle$	$\frac{1}{12\sqrt{10}}$	$-\frac{1}{12\sqrt{5}}$
$\langle B'\|D^{(8)}_{p3}\|B_{\overline{\mathbf{15}}}\rangle$	$-\frac{1}{2\sqrt{15}}$	$\frac{1}{\sqrt{30}}$
$\langle B'\|D^{(8)}_{p8}J_3\|B_{\overline{\mathbf{15}}}\rangle$	0	0
$\langle B'\|d_{ab3}D^{(8)}_{pa}J_b\|B_{\overline{\mathbf{15}}}\rangle$	$-\frac{1}{4\sqrt{15}}$	$\frac{1}{2\sqrt{30}}$

TABLE X. The matrix elements of the single and double Wigner D function operators when $a = 4 - i5$.

$B \to B'$	$\Xi_c^{\prime 0} \to \Lambda_c^+$	$\Omega_c^0 \to \Xi_c^+$	$\Xi_c^{*0} \to \Lambda_c^+$	$\Omega_c^{*0} \to \Xi_c^+$	$\Xi_c^{*+} \to \Sigma_c^{++}$	$\Omega_c^{*0} \to \Xi_c^{\prime +}$
$\langle B'\|D^{(8)}_{\Xi^-3}\|B\rangle$	$-\frac{1}{4\sqrt{3}}$	$\frac{1}{2\sqrt{6}}$	$\frac{1}{2\sqrt{6}}$	$-\frac{1}{2\sqrt{3}}$	$-\frac{1}{5\sqrt{2}}$	$-\frac{1}{5\sqrt{2}}$
$\langle B'\|D^{(8)}_{\Xi^-8}\hat{J}_3\|B\rangle$	0	0	0	0	$\frac{1}{5\sqrt{6}}$	$\frac{1}{5\sqrt{6}}$
$\langle B'\|d_{bc3}D^{(8)}_{\Xi^-b}\hat{J}_c\|B\rangle$	$\frac{1}{8\sqrt{3}}$	$-\frac{1}{4\sqrt{6}}$	$-\frac{1}{4\sqrt{6}}$	$\frac{1}{4\sqrt{3}}$	$\frac{1}{10\sqrt{2}}$	$\frac{1}{10\sqrt{2}}$
$\langle B'\|D^{(8)}_{83}D^{(8)}_{\Xi^-8}\|B\rangle$	$\frac{\sqrt{3}}{40}$	0	$-\frac{\sqrt{6}}{40}$	0	$\frac{1}{90\sqrt{2}}$	$\frac{1}{30\sqrt{2}}$
$\langle B'\|D^{(8)}_{88}D^{(8)}_{\Xi^-3}\|B\rangle$	$-\frac{1}{40\sqrt{3}}$	$-\frac{1}{10\sqrt{6}}$	$\frac{1}{20\sqrt{6}}$	$\frac{1}{10\sqrt{3}}$	$\frac{1}{90\sqrt{2}}$	$\frac{1}{30\sqrt{2}}$
$\langle B'\|d_{bc3}D^{(8)}_{8c}D^{(8)}_{\Xi^-b}\|B\rangle$	$\frac{1}{40}$	$-\frac{1}{20\sqrt{2}}$	$-\frac{1}{20\sqrt{2}}$	$\frac{1}{20}$	$\frac{7}{90\sqrt{6}}$	$\frac{1}{30\sqrt{6}}$

TABLE XI. The transition matrix elements of the single Wigner D function operators coming from the $\overline{15}$-plet component of the baryon wave functions when $a = 4 - i5$.

$B \to B'$	$\Xi_c^{\prime 0} \to \Lambda_c^+$	$\Omega_c^0 \to \Xi_c^+$	$\Xi_c^{*0} \to \Lambda_c^+$	$\Omega_c^{*0} \to \Xi_c^+$	$\Xi_c^{*+} \to \Sigma_c^{++}$	$\Omega_c^{*0} \to \Xi_c^{\prime +}$
$\langle B'_{\overline{\mathbf{15}}}\|D^{(8)}_{\Xi^-3}\|B\rangle$	$\frac{1}{4\sqrt{15}}$	$-\frac{1}{6\sqrt{10}}$	$-\frac{1}{2\sqrt{30}}$	$\frac{1}{6\sqrt{5}}$	$\frac{1}{9\sqrt{5}}$	$\frac{1}{3\sqrt{30}}$
$\langle B'_{\overline{\mathbf{15}}}\|D^{(8)}_{\Xi^-8}J_3\|B\rangle$	0	0	0	0	$\frac{1}{3\sqrt{15}}$	$\frac{1}{3\sqrt{10}}$
$\langle B'_{\overline{\mathbf{15}}}\|d_{ab3}D^{(8)}_{\Xi^-a}J_b\|B\rangle$	$\frac{3}{8\sqrt{15}}$	$-\frac{1}{4\sqrt{10}}$	$-\frac{3}{4\sqrt{30}}$	$\frac{1}{4\sqrt{5}}$	$\frac{1}{18\sqrt{5}}$	$\frac{1}{6\sqrt{30}}$
$\langle B'\|D^{(8)}_{\Xi^-3}\|B_{\overline{\mathbf{15}}}\rangle$	$-\frac{1}{4\sqrt{5}}$	0	$\frac{1}{2\sqrt{10}}$	0	$\frac{1}{9\sqrt{30}}$	0
$\langle B'\|D^{(8)}_{\Xi^-8}J_3\|B_{\overline{\mathbf{15}}}\rangle$	0	0	0	0	$\frac{1}{9\sqrt{10}}$	0
$\langle B'\|d_{ab3}D^{(8)}_{\Xi^-a}J_b\|B_{\overline{\mathbf{15}}}\rangle$	$-\frac{1}{8\sqrt{5}}$	0	$\frac{1}{4\sqrt{10}}$	0	$\frac{1}{18\sqrt{30}}$	0

TABLE XII. The transition matrix elements of the single Wigner D function operators coming from the $\overline{24}$-plet component of the baryon wave functions when $a = 4 - i5$.

$B \to B'$	$\Xi_c^{*+} \to \Sigma_c^{++}$	$\Omega_c^{*0} \to \Xi_c'^{+}$
$\langle B'_{\overline{\mathbf{24}}}\|D^{(8)}_{\Xi^-3}\|B\rangle$	$\frac{\sqrt{2}}{45}$	$\frac{1}{30\sqrt{3}}$
$\langle B'_{\overline{\mathbf{24}}}\|D^{(8)}_{\Xi^-8}J_3\|B\rangle$	$-\frac{2\sqrt{2}}{15\sqrt{3}}$	$-\frac{1}{15}$
$\langle B'_{\overline{\mathbf{24}}}\|d_{ab3}D^{(8)}_{\Xi^-a}J_b\|B\rangle$	$\frac{2\sqrt{2}}{45}$	$\frac{1}{15\sqrt{3}}$
$\langle B'\|D^{(8)}_{\Xi^-3}\|B_{\overline{\mathbf{24}}}\rangle$	$-\frac{1}{45\sqrt{3}}$	$-\frac{1}{30\sqrt{3}}$
$\langle B'\|D^{(8)}_{\Xi^-8}J_3\|B_{\overline{\mathbf{24}}}\rangle$	$\frac{2}{45}$	$\frac{1}{15}$
$\langle B'\|d_{ab3}D^{(8)}_{\Xi^-a}J_b\|B_{\overline{\mathbf{24}}}\rangle$	$-\frac{2}{45\sqrt{3}}$	$-\frac{1}{15\sqrt{3}}$

[1] P. A. Zyla *et al.* (Particle Data Group), Prog. Theor. Exp. Phys. **2020**, 083C01 (2020).
[2] K. U. Can, G. Erkol, B. Isildak, M. Oka, and T. T. Takahashi, J. High Energy Phys. 05 (2014) 125.
[3] H. Bahtiyar, K. U. Can, G. Erkol, and M. Oka, Phys. Lett. B **747**, 281 (2015).
[4] H. Bahtiyar, K. U. Can, G. Erkol, M. Oka, and T. T. Takahashi, Phys. Lett. B **772**, 121 (2017).
[5] H. Bahtiyar, K. U. Can, G. Erkol, M. Oka, and T. T. Takahashi, J. Phys. Soc. Jpn. Conf. Proc. **26**, 022027 (2019).
[6] R. Aaij *et al.* (LHCb Collaboration), Phys. Rev. Lett. **109**, 172003 (2012).
[7] R. Aaij *et al.* (LHCb Collaboration), Phys. Rev. Lett. **110**, 182001 (2013).
[8] R. Aaij *et al.* (LHCb Collaboration), Phys. Rev. Lett. **113**, 032001 (2014).
[9] R. Aaij *et al.* (LHCb Collaboration), Phys. Rev. Lett. **113**, 242002 (2014).
[10] R. Aaij *et al.* (LHCb Collaboration), Phys. Rev. Lett. **114**, 062004 (2015).
[11] R. Aaij *et al.* (LHCb Collaboration), Phys. Rev. Lett. **118**, 182001 (2017).
[12] R. Aaij *et al.* (LHCb Collaboration), Phys. Rev. D **102**, 071101 (2020).
[13] R. Aaij *et al.* (LHCb Collaboration), Phys. Rev. D **104**, L091102 (2021).
[14] N. Isgur and M. B. Wise, Phys. Lett. B **232**, 113 (1989).
[15] N. Isgur and M. B. Wise, Phys. Rev. Lett. **66**, 1130 (1991).
[16] H. Georgi, Phys. Lett. B **240**, 447 (1990).
[17] Gh.-S. Yang, H.-Ch. Kim, M. V. Polyakov, and M. Praszałowicz, Phys. Rev. D **94**, 071502 (2016).
[18] D. Diakonov, arXiv:1003.2157.
[19] E. Witten, Nucl. Phys. **B160**, 57 (1979).
[20] E. Witten, Nucl. Phys. **B223**, 433 (1983).
[21] W. Pauli and S. M. Dancoff, Phys. Rev. **62**, 85 (1942).
[22] T. H. R. Skyrme, Proc. R. Soc. A **260**, 127 (1961).
[23] D. Diakonov, V. Y. Petrov, and P. V. Pobylitsa, Nucl. Phys. **B306**, 809 (1988).
[24] M. Wakamatsu and H. Yoshiki, Nucl. Phys. **A524**, 561 (1991).
[25] D. Diakonov, arXiv:hep-ph/9802298.
[26] H.-Ch. Kim, M. V. Polyakov, and M. Praszalowicz, Phys. Rev. D **96**, 014009 (2017).
[27] H.-Ch. Kim, M. V. Polyakov, M. Praszalowicz, and G. S. Yang, Phys. Rev. D **96**, 094021 (2017); **97**, 039901(E) (2018).
[28] J. Y. Kim, H.-Ch. Kim, and G. S. Yang, Phys. Rev. D **98**, 054004 (2018).
[29] J. Y. Kim and H.-Ch. Kim, Prog. Theor. Exp. Phys. **2020**, 043D03 (2020).
[30] G. S. Yang and H.-Ch. Kim, Phys. Lett. B **808**, 135619 (2020).
[31] G. S. Yang and H.-Ch. Kim, Phys. Lett. B **781**, 601 (2018).
[32] G. S. Yang and H.-Ch. Kim, Phys. Lett. B **801**, 135142 (2020).
[33] J. Y. Kim and H.-Ch. Kim, Phys. Rev. D **97**, 114009 (2018).
[34] J. Y. Kim and H.-Ch. Kim, Prog. Theor. Exp. Phys. **2021**, 023D02 (2021).
[35] J. Y. Kim and H.-Ch. Kim, Prog. Theor. Exp. Phys. **2021**, 063D03 (2021).
[36] J. Y. Kim, H.-Ch. Kim, G. S. Yang, and M. Oka, Phys. Rev. D **103**, 074025 (2021).
[37] J. Y. Kim, H.-Ch. Kim, M. V. Polyakov, and H. D. Son, Phys. Rev. D **103**, 014015 (2021).
[38] T. M. Yan, H. Y. Cheng, C. Y. Cheung, G. L. Lin, Y. C. Lin, and H. L. Yu, Phys. Rev. D **46**, 1148 (1992); **55**, 5851(E) (1997).
[39] M. Q. Huang, Y. B. Dai, and C. S. Huang, Phys. Rev. D **52**, 3986 (1995); **55**, 7317(E) (1997).
[40] D. Pirjol and T. M. Yan, Phys. Rev. D **56**, 5483 (1997).
[41] H. Y. Cheng and C. K. Chua, Phys. Rev. D **92**, 074014 (2015).
[42] J. L. Rosner, Phys. Rev. D **52**, 6461 (1995).

[43] S. Tawfiq, P. J. O'Donnell, and J. G. Korner, Phys. Rev. D **58**, 054010 (1998).
[44] M. A. Ivanov, J. G. Korner, V. E. Lyubovitskij, and A. G. Rusetsky, Phys. Rev. D **60**, 094002 (1999).
[45] C. Albertus, E. Hernandez, J. Nieves, and J. M. Verde-Velasco, Phys. Rev. D **72**, 094022 (2005).
[46] H. Nagahiro, S. Yasui, A. Hosaka, M. Oka, and H. Noumi, Phys. Rev. D **95**, 014023 (2017).
[47] C. Chen, X. L. Chen, X. Liu, W. Z. Deng, and S. L. Zhu, Phys. Rev. D **95**, 014023 (2017).
[48] K. Azizi, M. Bayar, and A. Ozpineci, Phys. Rev. D **79**, 056002 (2009).
[49] K. U. Can, G. Erkol, M. Oka, and T. T. Takahashi, Phys. Lett. B **768**, 309 (2017).
[50] C. V. Christov, A. Blotz, H.-Ch. Kim, P. Pobylitsa, T. Watabe, T. Meissner, E. Ruiz Arriola, and K. Goeke, Prog. Part. Nucl. Phys. **37**, 91 (1996).
[51] J. M. Suh, Y. S. Jun, and H.-Ch. Kim, Phys. Rev. D **105**, 114040 (2022).
[52] S. L. Adler, Ann. Phys. (N.Y.) **50**, 189 (1968).
[53] W. Rarita and J. Schwinger, Phys. Rev. **60**, 61 (1941).
[54] H.-Ch. Kim, J. Korean Phys. Soc. **73**, 165 (2018).
[55] J. Yelton *et al.* (Belle Collaboration), Phys. Rev. D **104**, 052003 (2021).
[56] H. Y. Cheng and C. K. Chua, Phys. Rev. D **75**, 014006 (2007).
[57] A. Blotz, D. Diakonov, K. Goeke, N. W. Park, V. Petrov, and P. V. Pobylitsa, Nucl. Phys. **A555**, 765 (1993).
[58] H. Yabu and K. Ando, Nucl. Phys. **B301**, 601 (1988).
[59] H.-Ch. Kim, A. Blotz, M. V. Polyakov, and K. Goeke, Phys. Rev. D **53**, 4013 (1996).
[60] H.-Ch. Kim, M. Praszalowicz, and K. Goeke, Phys. Rev. D **57**, 2859 (1998).
[61] H.-Ch. Kim, M. V. Polyakov, M. Praszalowicz, and K. Goeke, Phys. Rev. D **57**, 299 (1998).
[62] T. Ledwig, A. Silva, H.-Ch. Kim, and K. Goeke, J. High Energy Phys. 07 (2008) 132.
[63] U. G. Meissner, N. Kaiser, and W. Weise, Nucl. Phys. **A466**, 685 (1987).
[64] T. Ledwig, A. Silva, and M. Vanderhaeghen, Phys. Rev. D **79**, 094025 (2009).
[65] J. M. Link *et al.* (FOCUS Collaboration), Phys. Lett. B **525**, 205 (2002).
[66] M. Artuso *et al.* (CLEO Collaboration), Phys. Rev. D **65**, 071101 (2002).
[67] Y. Kato *et al.* (Belle Collaboration), Phys. Rev. D **89**, 052003 (2014).
[68] S. H. Lee *et al.* (Belle Collaboration), Phys. Rev. D **89**, 091102 (2014).
[69] G. S. Yang and H.-Ch. Kim, Phys. Lett. B **785**, 434 (2018).